Atomic Data and Nuclear Data Tables 154 (2023) 101587

Contents lists available at ScienceDirect

Atomic Data and Nuclear Data Tables

journal homepage: www.elsevier.com/locate/adt

Systematic study of fusion barriers with energy dependent barrier radius

Yeruoxi Chen [a], Hong Yao [a,b], Min Liu [a,c], Junlong Tian [a,c], Peiwei Wen [d], Ning Wang [a,c,*]

[a] Department of Physics, Guangxi Normal University, Guilin 541004, PR China
[b] School of Physics, Beihang University, Beijing 102206, PR China
[c] Guangxi Key Laboratory of Nuclear Physics and Technology, Guilin 541004, PR China
[d] China Institute of Atomic Energy, Beijing 102413, PR China

ARTICLE INFO

Article history:
Received 7 April 2023
Received in revised form 9 May 2023
Accepted 11 May 2023
Available online 31 May 2023

Dataset link: http://www.imqmd.com/fusion/MSW_barrier.txt

Keywords:
Fusion cross section
Coulomb barrier
Barrier parameters
de Broglie wavelength

ABSTRACT

Considering energy dependence of the barrier radius in heavy-ion fusion reactions, a modified Siwek-Wilczyński (MSW) fusion cross section formula is proposed. With the MSW formula, the fusion barrier parameters for 367 reaction systems are systematically extracted, based on 443 datasets of measured cross sections. We find that the fusion excitation functions for about 60% reaction systems can be better described by introducing the energy dependence of the barrier radius which is due to the dynamical effects at energies near and below the barrier. Considering both the influence of the geometry radii and that of the reduced de Broglie wavelength of the colliding nuclei, the barrier heights are well reproduced with only one model parameter. The extracted barrier radius parameters linearly decrease with the effective fissility parameter, and the width of the barrier distribution relates to the barrier height, as well as the reduced de Broglie wavelength at energies around the Coulomb barrier.

* Corresponding author at: Department of Physics, Guangxi Normal University, Guilin 541004, PR China.
E-mail address: wangning@gxnu.edu.cn (N. Wang).

https://doi.org/10.1016/j.adt.2023.101587

Contents

1. Introduction

The problem of overcoming a potential barrier is of importance not only in nuclear physics, but also in many other fields of the nature sciences. Knowledge of the nucleus–nucleus interaction potential is an essential ingredient in the analysis of elastic and inelastic scattering, as well as of fusion reactions between nuclei. The information concerning the potential barrier is of crucial importance for the synthesis of super-heavy nuclei and heavy-ion fusion at deep sub-barrier energies which has attracted a great deal of attention in recent years [1–10]. Up to now, the fusion cross sections for more than a thousand of reaction systems have been measured in the past several decades. A systematic study of the fusion barriers based on these data is therefore interesting and necessary.

Classically a particle can only overcome a potential barrier when its total energy exceeds the barrier height. In the classical description of fusion excitation functions, the fusion cross section $\sigma_{\rm fus}(E)$ at a center-of-mass incident energy E is given by

$$\sigma_{\rm fus}(E) = \pi R_B^2 (1 - V_B/E), \tag{1}$$

where R_B is the barrier radius and V_B is the barrier height. The barrier parameters are obtained from the data by fitting a straight line through a plot of $\sigma_{\rm fus}$ vs $1/E$. The slope and intercept of this line with the $1/E$ axis lead to the barrier radius and height, respectively. At energies below the barrier, the particle may tunnel through the potential barrier, as a consequence of quantum mechanics. This tunneling effect was first recognized in the 1920's and the α-decay of nuclei was explained as a tunneling effect [11]. In the 1970's, the fusion cross sections are analytically described by the well known Wong formula [12], based on the assumption of a parabolic barrier together with the barrier penetration concept,

$$\sigma_{\rm fus}(E) = \frac{\hbar\omega}{2E} R_B^2 \ln\{1 + \exp[2\pi(E - V_B)/\hbar\omega]\}, \tag{2}$$

where, $\hbar\omega$ is the s-wave barrier curvature. The energy dependence of the barrier curvature is introduced in Ref. [13] for a better description of the fusion cross sections at deeply sub-barrier energies. For relatively large values of E, the result of Wong formula reduces to the classical formula Eq. (1).

For the sub-barrier fusion reactions leading to heavy compound nuclei, an important observation is that the measured fusion cross sections exhibit strong enhancements compared to estimations using a simple one-dimensional barrier penetration model [8]. These enhancements have been accounted for in terms of strong couplings between the relative motion of colliding nuclei and the intrinsic degrees of freedom, such as the collective vibrations of nuclei and nucleon transfer in the neck region. To consider the coupling effects, Stelson introduced a distribution of barrier heights $D(B)$ in the calculation of the fusion excitation function around 1990 [14,15],

$$\sigma_{\rm fus}(E) = \int D(B)\sigma_{\rm fus}^{(1)}(E, B)dB, \tag{3}$$

with $\int D(B)dB = 1$. Here, $\sigma_{\rm fus}^{(1)}(E, B)$ is the fusion cross section based on a single barrier with a height B.

To describe $D(B)$, a single-Gaussian distribution of barrier heights predicted from different orientations of colliding nuclei undergoing slow deviations from sphericity is used by Siwek-Wilczyńska and Wilczyński (SW). Together with Eq. (1) for describing $\sigma_{\rm fus}^{(1)}(E, B)$, the SW formula was proposed [16]. With the SW formula, the heavy-ion fusion cross sections for 29 systems, from ^{16}O+^{18}O to ^{64}Ni+^{124}Sn, at extreme sub-barrier energies have been analyzed [17]. Very recently, Wen et al. applied the SW formula to systematically extract the barrier information from the experimental fusion excitation functions, and found that the SW formula behaves much better for the barrier fitting than the Wong formula [18]. In addition to the single-Gaussian function for describing $D(B)$, two-Gaussian function [19,20], asymmetric Gaussian function [21,22] and as well as multi-Gaussian function [23,24] are also frequently used. The experimental barrier height distribution $D(E)$ can be extracted from a precise experiment of the fusion excitation function via the second derivative [25,26]:

$$D(E) = \frac{1}{\pi R_B^2} \frac{d^2\,(E\sigma_{\rm fus})}{dE^2}. \tag{4}$$

The validity of all these analyses mentioned above requires that all l waves contributing to the fusion cross section have the same barrier radius R_B, a condition which is probably not fulfilled for most reactions [27]. The energy dependence of the nucleus–nucleus potential was clearly observed from some microscopic dynamics calculations, such as the simulations based on the time-dependent Hartree–Fock (TDHF) theory [28,29] and the improved quantum molecular dynamic (ImQMD) model [30,31], due to the strong dynamical effects in fusion process. For fusion reactions with deformed nuclei, the orientation of the colliding nuclei significantly influences not only the barrier height but also the barrier radius. For tip–tip configuration in fusion reaction induced by prolate nuclei, one obtains a larger barrier radius, comparing with that for side–side configuration [29,32]. It is therefore necessary to investigate the influence of energy and orientation dependence of the barrier radius on the fusion cross sections.

The purpose of the present work is to systematically extract the fusion barriers based on the SW formula together with the energy dependence of the barrier radius being considered. The structure of this paper is as follows: In Section 2, energy dependence of the barrier radius for ^{16}O+^{208}Pb and ^{34}S+^{168}Er will be investigated. In Section 3, a modified SW formula will be proposed and the model accuracy for describing some fusion

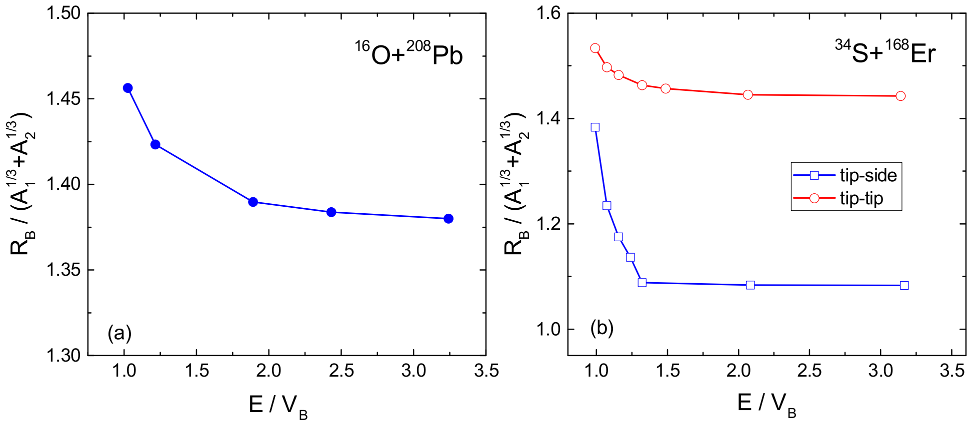

Fig. 1. Barrier radius as a function of E/V_B for ^{16}O+^{208}Pb (a) and ^{34}S+^{168}Er (b) from the TDHF calculations. A_1 and A_2 denote the mass number of projectile and target nuclei, respectively. V_B in horizontal axis are taken from a linear fit of the measured σ_{fus} [33,34] vs $1/E$ in the region larger than 100 mb.

excitation functions will be tested. In Section 4, the information concerning fusion barriers extracted from 443 datasets of experimental data for 367 different projectile–target combinations, will be presented and the systematics of the fusion barrier will also be analyzed. Finally, a summary will be given in Section 5.

2. Energy dependence of barrier radius

To investigate the energy dependence of barrier radius, we firstly use the time dependent Hartree–Fock (TDHF) theory for simulating the fusion reactions ^{16}O+^{208}Pb and ^{34}S+^{168}Er. The nucleus–nucleus interaction potential is extracted by using the density-constrained TDHF approach [32,35]. In ^{34}S+^{168}Er, the tip–tip and tip–side orientations for the deformed reaction partners are taken into account. The Skyrme SLy4d interactions [26] are used by static HF and TDHF dynamic evolution, in which the numerical boxes are chosen as $30 \times 30 \times 30$ fm^3 and $30 \times 30 \times 50$ fm^3, respectively. The time propagation is carried out using a Taylor-series expansion up to the sixth order of the unitary mean-field propagator with a time step of 0.2 fm/c, and the initial distance of two nuclei is set to 20 fm.

In Fig. 1, we show the calculated barrier radii at different incident energies for ^{16}O+^{208}Pb and ^{34}S+^{168}Er, which are scaled by $A_1^{1/3} + A_2^{1/3}$ to see the radius parameter. One can see that for both reactions at energies around the barrier height V_B, the barrier radius decrease evidently with incident energy. Especially for ^{34}S+^{168}Er at tip-side orientation, the radius parameter falls sharply with energy, from 1.4 fm at $E \approx V_B$ down to 1.1 fm at $E \approx 1.3V_B$. At energies much higher than the barrier height, the barrier radius does not change too much. The energy dependence of the barrier radius is due to the dynamical effects in fusion process. At energies around the barrier height, the fusion process is relatively slow and the reaction partners have enough time to readjust nuclear density distributions of the reaction system. The dynamical deformation of the densities and neutron transfer in the neck region can result in the enlargement of the barrier radius and the reduction of barrier height correspondingly.

In addition to the TDHF calculations, the barrier radius is also analyzed based on the measured fusion excitation function. According to Eq. (1), the barrier radius can be expressed as,

$$R_B(E) = \left[\frac{\sigma_{\text{fus}}}{\pi(1 - V_B/E)}\right]^{1/2}. \tag{5}$$

In Fig. 2, we show the extracted barrier radius for ^{16}O+^{208}Pb and ^{34}S+^{168}Er, based on the measured fusion excitation function σ_{fus} [33,34]. At energies above the fusion barrier, the barrier radius does not change significantly with incident energy. At sub-barrier energies, the enhancement of the barrier radius can be clearly observed. In Ref. [36], a generalized Wong formula is proposed by Rowley and Hagino through considering energy dependence of the barrier parameters. The trend of the energy dependence for barrier radius observed in Fig. 2 is generally in agreement with those from the TDHF calculations and the generalized Wong formula.

Both the TDHF calculations and the data analysis imply that the assumption used in the traditional formula, i.e., all l waves contributing to the fusion cross section having the same barrier radius R_B, is generally valid at energies above the barrier height. However, at energies around the barrier, the enhancement of barrier radius due to dynamical effects should be considered for a better description of the fusion excitation functions. To consider the influence of the dynamical effects on barrier radius, we empirically introduce a correction term to the traditional barrier radius R_0,

$$R_B(X) = R_0 + \Delta R \exp(-X) \operatorname{erfc}(X). \tag{6}$$

The definition of X and the determination of the correction factor ΔR will be discussed later. The solid curves in Fig. 2 denote the results according to Eq. (6). Comparing with the results of SW formula, the trend of energy dependence for the barrier radius can be much better described by using Eq. (6), especially at sub-barrier energies.

3. Modified Siwek-Wilczyński formula and some tests

Considering the energy dependence of the barrier radius given by Eq. (6), we propose a modified Siwek-Wilczyński (MSW) formula for describing the fusion excitation function

$$\sigma_{\text{fus}}(E) = \pi R_B^2(X) \frac{W}{\sqrt{2}E}[X \operatorname{erfc}(-X) + \frac{1}{\sqrt{\pi}} \exp(-X^2)], \tag{7}$$

where $X = \frac{E-V_B}{\sqrt{2}W}$. V_B and W denote the centroid and the standard deviation of the Gaussian function, respectively. Together with the traditional barrier radius R_0 and the correction factor ΔR in Eq. (6), there are a total of four barrier parameters in the MSW formula. If $\Delta R = 0$, the result of Eq. (7) reduces to the standard SW formula [16]. For a certain fusion reaction, the four parameters in the MSW formula can be determined by fitting the measured fusion excitation function. The popular Minuit minimization program [39] is usually applied to determine the fitting parameters by searching the global minimum in the hypersurface of the χ^2 function. The χ^2 per energy point is expressed as

$$\chi^2_{pt} = \frac{1}{N}\sum_{i=1}^{N}\left[\frac{\sigma_{\text{th}}(E_i) - \sigma_{\text{exp}}(E_i)}{\delta\sigma_{\text{exp}}(E_i)}\right]^2, \tag{8}$$

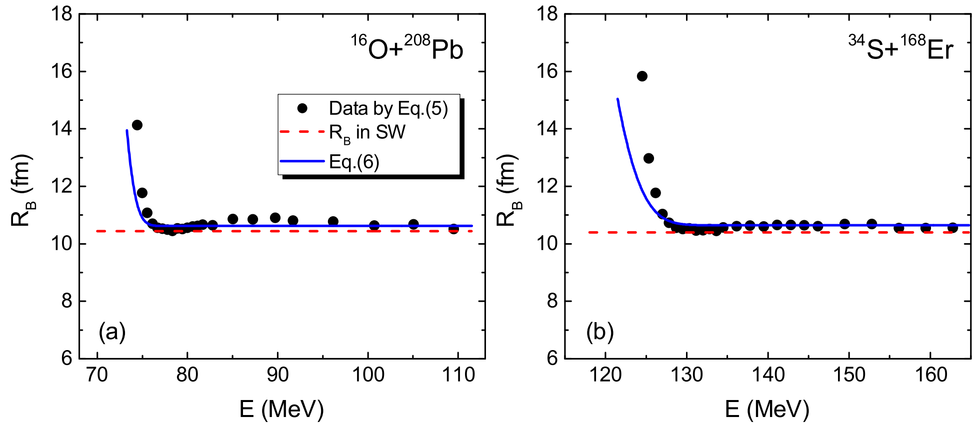

Fig. 2. Barrier radius for $^{16}O+^{208}Pb$ (a) and $^{34}S+^{168}Er$ (b) from the measured fusion excitation functions. The circles denote the extracted results from the data by using Eq. (5). The dashed lines denote the results of SW formula. The solid curves denote the results of Eq. (6).

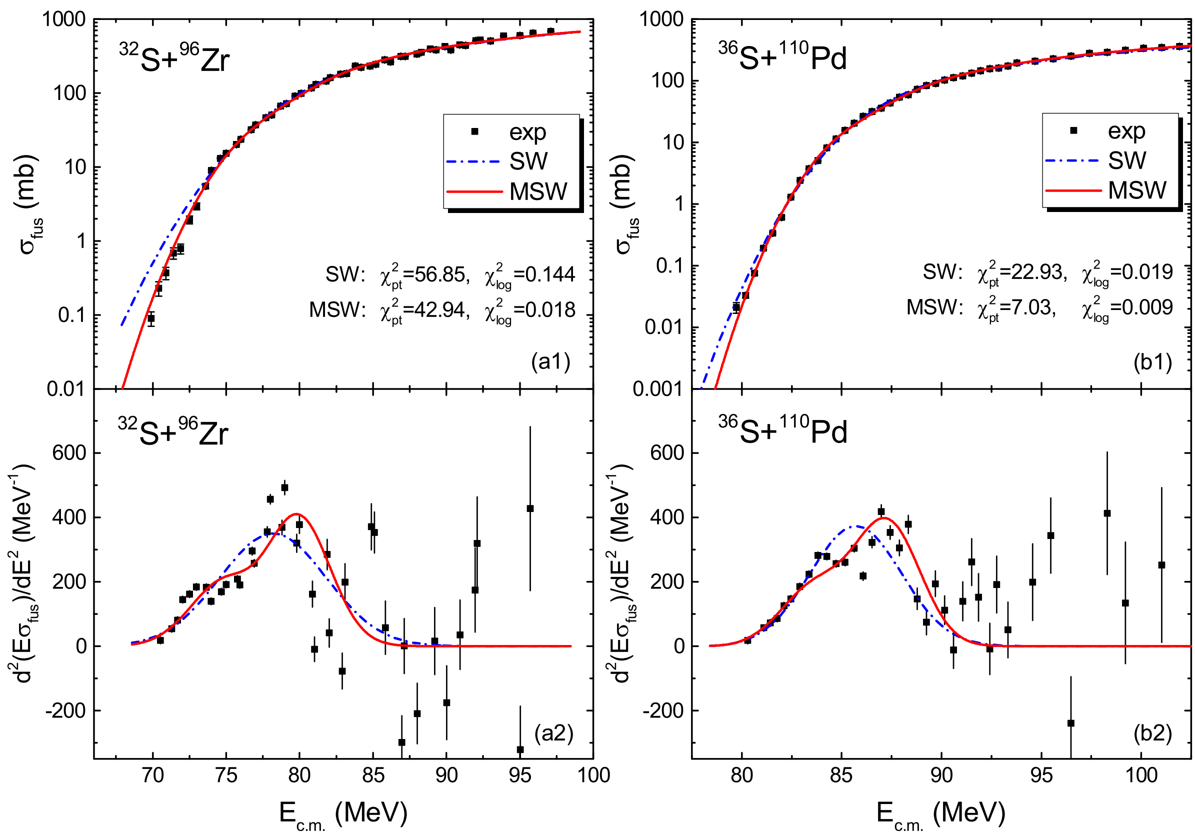

Fig. 3. (Color online) Fusion excitation functions and fusion barrier distributions for $^{32}S+^{96}Zr$ and $^{36}S+^{110}Pd$. The squares in (a1) and (b1) denote the experimental data taken from [37,38] for $^{32}S+^{96}Zr$ and $^{36}S+^{110}Er$, respectively. The squares in (a2) and (b2) denote the extracted barrier distribution according to Eq. (4). The dash-dotted curve and the solid curve denote the results of SW formula and those of MSW formula, respectively.

in which the uncertainty of fusion cross section is involved in the fitting process. In addition to χ^2_{pt}, the mean-square deviation between the measured fusion cross sections and model predictions is also frequently used to determine the best-fit model parameters [22,23]. Here, the mean-square deviation in logarithmic scale is defined as,

$$\chi^2_{\log} = \frac{1}{N}\sum_{i=1}^{N}\left[\log\left(\sigma_{\text{th}}\left(E_i\right)\right) - \log\left(\sigma_{\exp}\left(E_i\right)\right)\right]^2 . \tag{9}$$

$\chi^2_{\log}$ is more effective to check the trend of fusion cross sections at sub-barrier energies. In this work, we combine these two quantities and use $\bar{\chi} = (\chi^2_{pt} + \chi^2_{\log})^{1/2}$ to search for the best-fit parameters.

Figs. 3 and 4 show the fusion excitation functions and barrier distributions for $^{32}S+^{96}Zr$, $^{36}S+^{110}Pd$, $^{58}Ni+^{54}Fe$ and $^{58}Ni+^{60}Ni$ reactions. We note that introducing the energy dependence of barrier radius, the experimental data can be much better reproduced, especially for the fusion cross sections at deep sub-barrier energies. With the MSW formula, both χ^2_{pt} and $\chi^2_{\log}$ are significantly smaller than those with the SW formula. In addition, the barrier distributions are also studied to check the details in reproducing the fusion excitation functions. The distributions are extracted from the experimental excitation functions using the point-difference

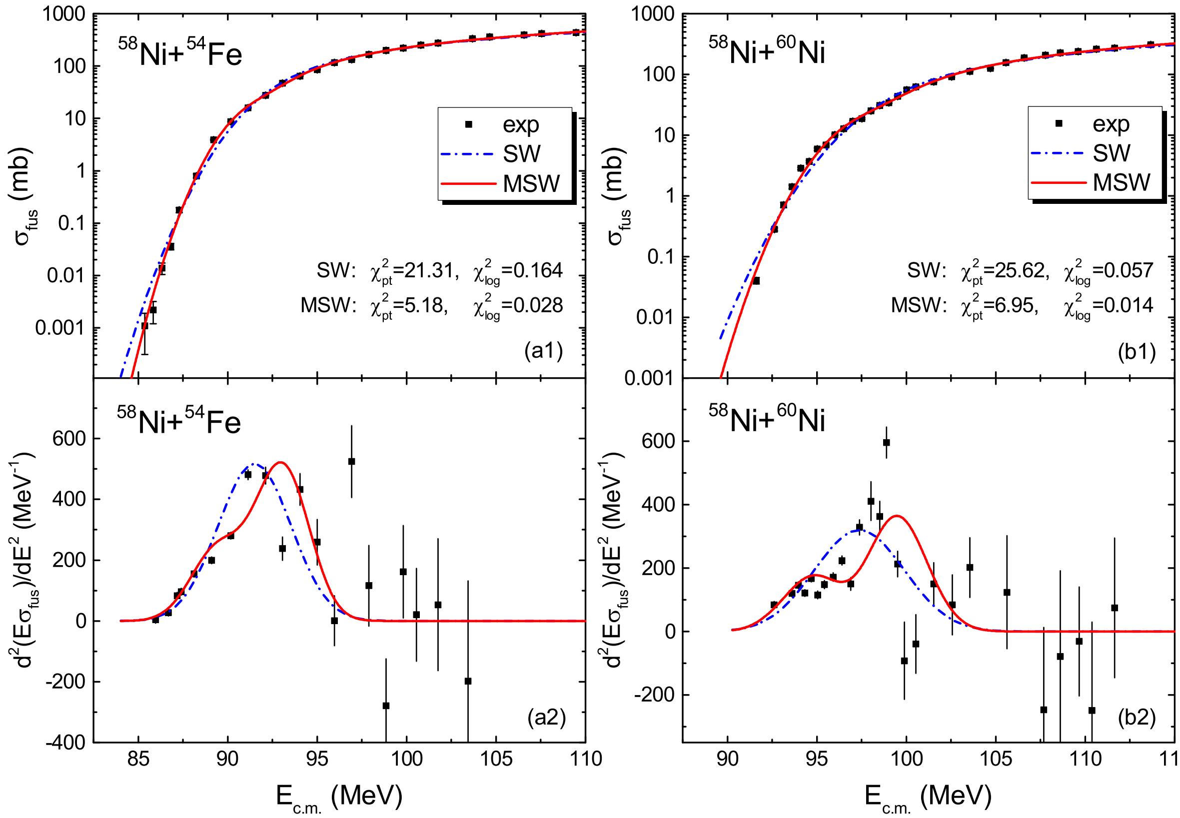

Fig. 4. (Color online) The same as Fig. 3, but for ^{58}Ni+^{54}Fe and ^{58}Ni+^{60}Ni.
Source: The experimental data are taken from [40,41].

approximation [26] according to Eq. (4),

$$\frac{d^2\,(E\sigma_{\rm fus})}{dE^2} \approx \frac{2E\sigma_{\rm fus}(E) - E\sigma_{\rm fus}(E+\Delta E) - E\sigma_{\rm fus}(E-\Delta E)}{(\Delta E)^2}, \quad (10)$$

with an energy step $\Delta E = 2.5$ MeV. From (a2) and (b2) in Figs. 3 and 4, one can see that with energy dependence of R_B, the left shoulders in the barrier distributions for these four systems can be evidently observed in the MSW calculations, although the single-Gaussian function is adopted in Eq. (3).

4. Extracted barrier parameters

Up to now, a large number of fusion excitation functions have been measured in the past several decades. Most of data for the fusion cross sections including fusion–fission and evaporation residue obtained from the tables or the graphs of the corresponding publications, are collected in the NRV website [42]. In this work, we use a similar procedure as adopted in Ref. [18] to select the experimental fusion data. In addition to the data in the NRV website, some fusion excitation functions measured in very recent years are also collected in this work. One usually defines the fusion cross section $\sigma_{\rm fus}$ as a sum of evaporation residue cross section $\sigma_{\rm EvR}$ and fission cross section $\sigma_{\rm FF}$. For light and intermediate mass systems, it is thought that $\sigma_{\rm fus} \simeq \sigma_{\rm EvR}$, since the fission barrier of the compound nuclei is high enough and the fission cross sections could be negligible. For heavy systems, e.g. the reactions leading to lanthanides or heavier nuclei, the contribution of fission cannot be ignored, the fission cross sections need to be included in $\sigma_{\rm fus}$. For fusion reactions leading to actinides, the evaporation residue cross sections are relatively small and the fission cross sections play a dominant role in the extraction of the fusion barrier. For fusion reactions leading to super-heavy nuclei, the evaporation residues become negligible and the quasi-fission cross sections are dominant in the total capture cross sections with which the Coulomb barrier can be extracted. For some systems with the same projectile–target combination, the data from different experimental groups are slightly different and the fusion barrier is separately analyzed and presented in this work.

Firstly, we analyze the 29 fusion reaction systems mentioned in Ref. [17], where Jiang et al. systematically analyzed the fusion cross sections for the 29 systems by using the SW formula. In Fig. 5, we compare the results from the SW formula and those from the MSW formula proposed in this work. From Fig. 5(a), one notes that for most of reactions, the χ^2_{pt} values with the MSW formula are much smaller than those with SW formula, since one more parameter ΔR is involved. For the lightest system ^{16}O+^{18}O, the obtained barrier parameters from the two formulas are very close to each other, although the obtained χ^2_{pt} in this work is larger than that in Ref. [17]. The obtained barrier heights from the two formulas are in good agreement with each other. The discrepancies in W and R_0 are within 25%, which indicates that the introduction of the correction factor ΔR in the MSW formula influences W and R_0 relatively larger than V_B.

Then, we systematically analyze a total of 443 datasets of measured fusion (and/or fission) cross sections for 367 different projectile–target combinations by using the MSW formula. The values of $\bar{\chi}$ corresponding to the best-fit parameters for all considered systems are simultaneously obtained. In Fig. 6, we show the distribution for the relative deviation of $\bar{\chi}$ between the results of MSW and those of SW, i.e., $(\bar{\chi}^{\rm SW} - \bar{\chi}^{\rm MSW})/\bar{\chi}^{\rm SW}$. We find that for 173 datasets, the relative deviation $\Delta\bar{\chi}/\bar{\chi}$ is smaller than 0.1%. For 122 datasets, the improvement is larger than 10% and for 148 datasets the values of $\Delta\bar{\chi}/\bar{\chi}$ are located in the region of 0.1%−10%. It indicates that the measured fusion excitation

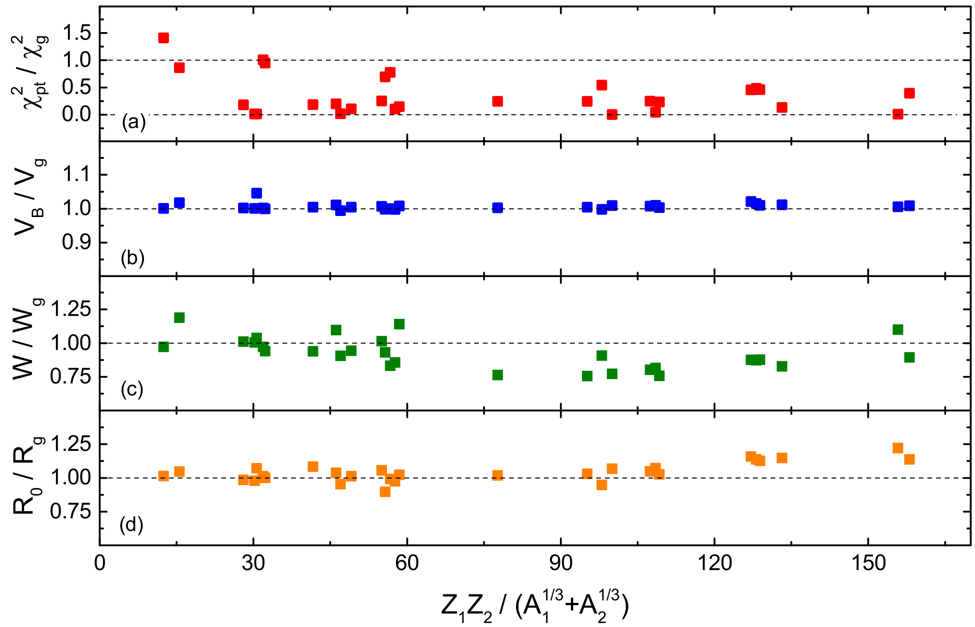

Fig. 5. (Color online) Ratios between the extracted barrier parameters in this work and those in Ref. [17]. χ_g^2, V_g, W_g and R_g denote the obtained χ_{pt}^2, the barrier height, the standard deviation and the barrier radius in Ref. [17], respectively.

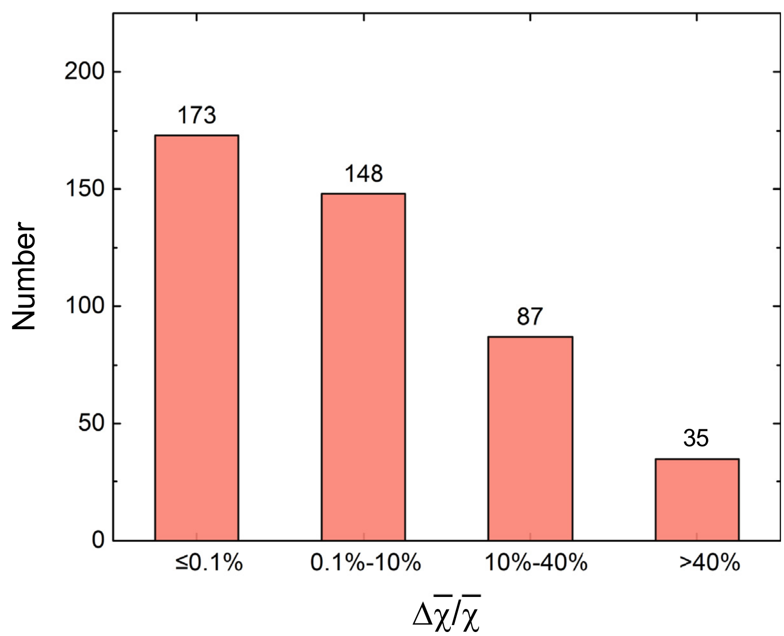

Fig. 6. (Color online) Distribution of the relative improvement in $\bar{\chi}$ by using MSW comparing with SW.

functions for about 60% reactions can be better reproduced by introducing the energy dependence of barrier radius into the SW formula. The extracted barrier parameters and the references for these systems are listed in Table A.

For studying the fusion of heavy nuclei, one usually introduces a parameter to describe the fissility of the reaction system. The effective fissility parameter is defined as,

$$x_{\text{eff}} = \frac{(Z^2/A)_{\text{eff}}}{(Z^2/A)_{\text{thr}}}, \tag{11}$$

with the effective fissility

$$(Z^2/A)_{\text{eff}} = \frac{4Z_1Z_2}{A_1^{1/3}A_2^{1/3}(A_1^{1/3}+A_2^{1/3})} \tag{12}$$

and the threshold [43] for the effective fissility $(Z^2/A)_{\text{thr}} \approx 33$, beyond which an extra push is needed to achieve fusion. Z_1 and Z_2 in Eq. (12) denote the charge numbers of the projectile and target nuclei, respectively.

Based on the extracted barrier height V_B, the radius of the corresponding Coulomb potential $R_{\text{Coul}} = Z_1Z_2e^2/V_B$ is systematically analyzed. In Fig. 7(a), we show the extracted radius parameter R_{Coul}. The decreasing trend of the radius parameter $R_{\text{Coul}}/(A_1^{1/3} + A_2^{1/3})$ with the effective fissility parameter x_{eff} can be evidently observed. To understand the physics behind, we also show in Fig. 7(b) the reduced de Broglie wavelength $\lambda\!\!\!^{-}_B = \hbar/\sqrt{2\mu V_B}$ of the colliding nuclei at an incident energy of $E = V_B$. μ is the reduced mass of the reaction system. One can see that $\lambda\!\!\!^{-}_B$ approaches to zero with the increase of x_{eff}, which indicates that the influence of

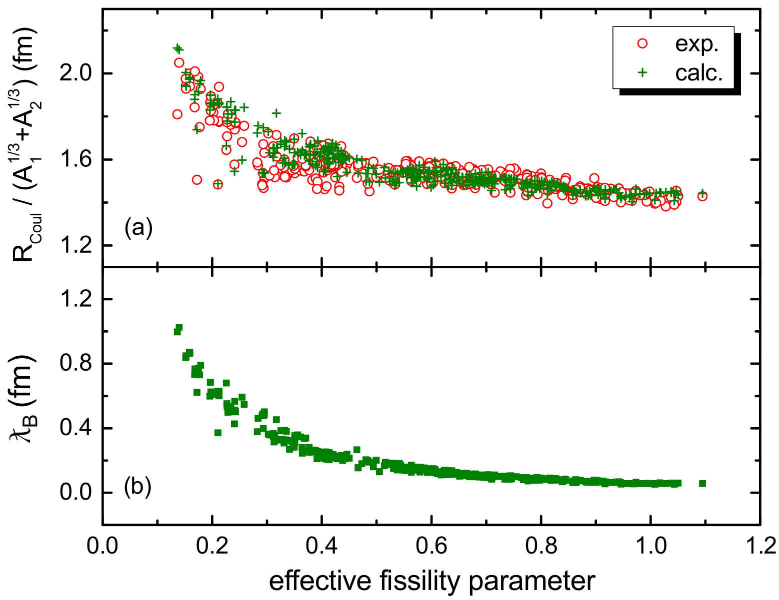

Fig. 7. (Color online) (a) Extracted radius parameter for the Coulomb potential as a function of the effective fissility parameter x_{eff}. The open circles and the crosses denote the data based on the extracted barrier heights and the calculated results by using Eq. (13), respectively. (b) Reduced de Broglie wavelength $ƛ_B$ of the colliding nuclei at an incident energy of $E = V_B$.

de Broglie wavelength is negligible for heavy fusion systems. It is known that the capture cross section $\sigma_{\text{cap}} \propto \pi(R+ƛ)^2$ considering the wave properties of incident particles. For heavy fusion system $ƛ$ is very small and consequently one obtains the traditional geometry cross section $\propto \pi R^2$. For very light fusion systems (with smaller values of x_{eff}) and thermal neutron induced capture cross sections, the contribution of $ƛ$ needs to be considered.

To describe the radius of the Coulomb potential R_{Coul}, we consider both the influence of the geometry radii of nuclei and that of the wave properties of particles. We write R_{Coul} as a sum of the charge radii of projectile and target nuclei, a parameter $d = 1.75$ fm which is related to the interaction range, and as well as the reduced de Broglie wavelength,

$$R_{\text{Coul}} = R_1^C + R_2^C + 1.75 + ƛ_B. \tag{13}$$

The charge radius $R^C \simeq \sqrt{\frac{5}{3}} r_{\text{ch}}$ of a nucleus neglecting its deformations is taken from the root-mean-square (rms) charge radius r_{ch} which can be measured with high precision [44–46]. In the calculations, the reduced de Broglie wavelength $ƛ_B = \hbar/\sqrt{2\mu V_B}$ can be obtained by using an iterative procedure with an initial value of $V_B \approx Z_1 Z_2 e^2/(R_1^C + R_2^C + 1.75)$. The calculated results of R_{Coul} are also shown in Fig. 7(a) for comparison. One sees that the extracted radius parameter can be well reproduced. It indicates that the decreasing trend of the barrier radius parameter could have a relationship with the de Broglie wavelength of the colliding nuclei. With only one parameter in Eq. (13), the extracted barrier heights can be well reproduced by using

$$V_B = Z_1 Z_2 e^2/R_{\text{Coul}}, \tag{14}$$

with an rms deviation of only 1.52 MeV for all considered reactions. The relative deviation $\Delta V_B = (V_B^{\text{exp}} - V_B^{\text{th}})/V_B^{\text{exp}}$ between data and model predictions is also calculated, the corresponding rms error is 2.83% with Eq. (14) for calculating V_B^{th}, which is much smaller than the corresponding value of 4.29% from the three-parameter WKJ formula in Ref. [47] and slightly smaller than that of 2.84% from the two-parameter MCW formula in Ref. [18].

The systematics of the extracted barrier radius R_0 and that of the standard deviation of the Gaussian function W are investigated simultaneously. In Fig. 8, we show the extracted barrier radius parameters $R_0/(A_1^{1/3} + A_2^{1/3})$ and the value W/V_B as functions of the effective fissility parameter x_{eff}. We note that the extracted barrier radius parameter linearly decreases with the effective fissility parameter, and the decreasing trend of W/V_B is very similar to that of $ƛ_B$ in Fig. 7(b). We therefore propose two formulas,

$$R_0 = (1.62 - 0.57x_{\text{eff}})(A_1^{1/3} + A_2^{1/3}) \tag{15}$$

and

$$W = (0.014 + 0.135ƛ_B)V_B, \tag{16}$$

for describing R_0 and W, respectively. The similar trends for the barrier radius and the distribution width are also observed in Ref. [17]. In addition to the influence of wave properties of reaction partners, the systematic decreasing trend of the barrier radius R_0 could also be due to the influence of quasi-fission of reaction systems, since the quasi-fission cross sections are not involved in the present analysis. The contribution of quasi-fission to the total capture cross sections may increase with x_{eff}. It is thought that the influence of quasi-fission becomes evident and an extra push is needed to achieve fusion for the systems with $x_{\text{eff}} > 1$ [43,48]. The systematics of the correction factor ΔR is unclear at the moment. The shell effects of reaction systems and the change of Q value due to nucleon transfer should be further investigated to explore the systematics of ΔR.

For fusion reactions with $\Delta R = 0$ listed in Table A, we systematically analyze the experimental data. Simultaneously, the fusion cross sections for these systems are also calculated for comparison by using the SW formula with Eqs. (14)–(16) for calculating V_B, R_0 and W. In Fig. 9, the measured cross sections scaled by πR_0^2 are shown as a function of X. We note that the cross sections for different reactions have a quite similar trend at sub-barrier and over-barrier energies. The experimental data can be reasonably well reproduced by the SW formula together with the proposed barrier parameter formulas.

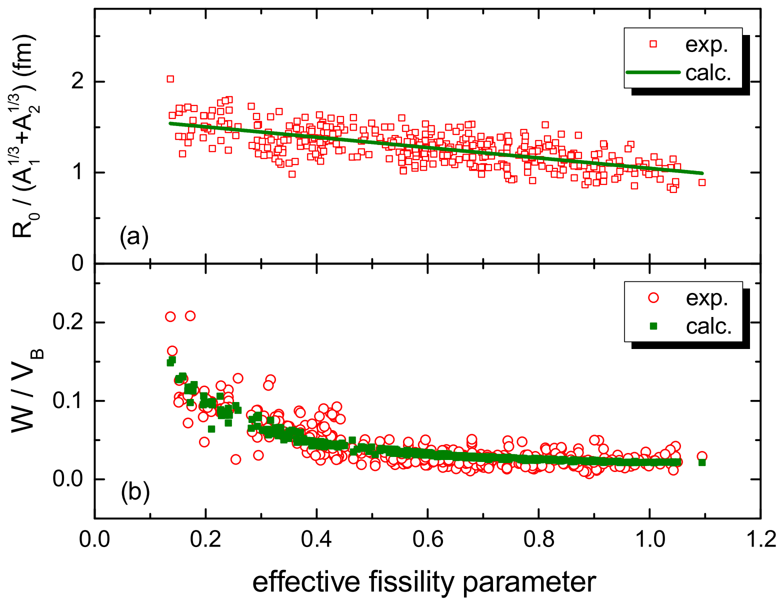

Fig. 8. (Color online) (a) Extracted barrier radius parameters as a function of the effective fissility parameter $x_{\rm eff}$. The line denotes a linear fit to the extracted results. (b) Standard deviation of the Gaussian function W divided by the corresponding barrier height V_B as a function of $x_{\rm eff}$. The circles denote the extracted results and the squares denote the predictions with Eq. (16).

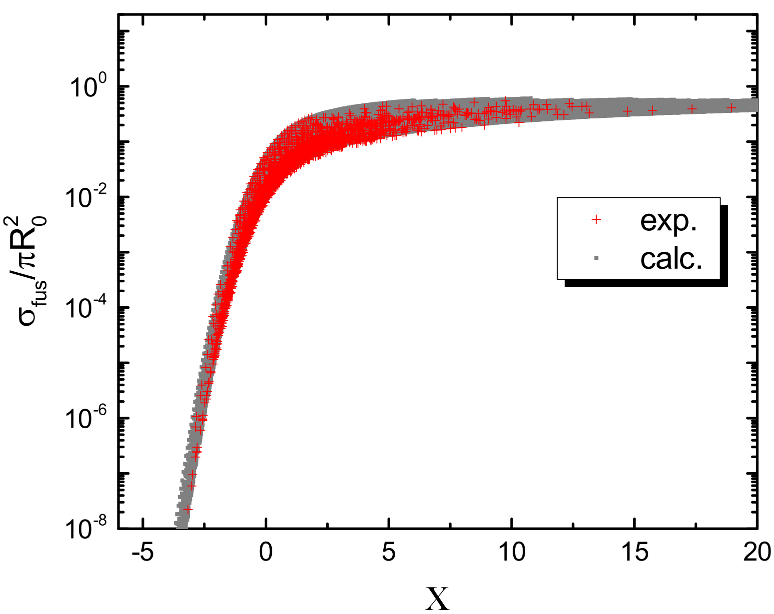

Fig. 9. (Color online) Measured cross sections for reactions with $\Delta R = 0$ as a function of $X = \frac{E-V_B}{\sqrt{2}W}$. Here, the cross sections are scaled by πR_0^2. Eqs. (14)–(16) are used in the calculations of V_B, R_0 and W, respectively. Squares denote the model predictions from the SW formula.

5. Summary

A total of 443 datasets of measured fusion (and/or fission) excitation functions for 367 different projectile–target combinations, are systematically analyzed by using a new fusion cross section formula, in which the energy-dependent barrier radius R_B is introduced into the Siwek-Wilczyński formula. We find that the fusion excitation functions for about 60% reaction systems can be better described by considering the energy dependence of R_B. The energy dependence of barrier radius can also be clearly observed from the time-dependent Hartree–Fock (TDHF) calculations, which is due to the dynamical effects at energies around the Coulomb barrier. With the energy dependence of R_B, the barrier distributions based on the double-differentiation process can be better reproduced for some systems, especially the left shoulder in the distribution. Considering both the influence of the geometry radii and that of the wave properties of the colliding nuclei, the barrier height V_B can be well reproduced with only one model parameter. We also note that the extracted barrier radius parameters linearly decrease with the effective fissility parameter, from about 1.6 fm for very light reaction systems to about 1.0 fm for heavy systems in which quasi-fission could occur. It seems that the width of the barrier distribution relates to the barrier height, as well as the reduced de Broglie wavelength of the colliding nuclei at energies around the Coulomb barrier.

Table A
Extracted barrier parameters based on 443 datasets of measured cross sections together with the MSW formula. V_B and W denote the centroid and the standard deviation of the Gaussian function for barrier distribution, respectively. R_0 denotes the traditional barrier radius. ΔR denotes the correction factor for the barrier radius. χ^2_{pt} denotes the χ^2 per energy point, and $\chi^2_{\log}$ denotes the mean-square deviation between data and predictions in logarithmic scale. EvR and FF are cross sections for fusion–evaporation residues and fusion–fission, respectively.

Reaction	V_B (MeV)	W (MeV)	R_0 (fm)	ΔR (fm)	χ^2_{pt}	$\chi^2_{\log}(\times 100)$	Type	Ref.
^{4}He+^{93}Nb	11.74	1.00	9.38	0.350	0.609	0.666	EvR	[49]
^{4}He+^{154}Sm	15.29	0.39	9.77	3.744	0.393	0.398	EvR	[50]
^{4}He+^{233}U	22.63	1.67	11.83	0.244	5.418	14.639	FF	[51]
^{4}He+^{235}U	23.28	2.06	10.49	0.003	0.041	0.042	FF	[52]
^{4}He+^{236}U	22.25	1.59	10.55	0	0.169	0.124	FF	[53]
^{4}He+^{238}U	22.90	1.67	12.57	0.242	4.341	9.856	FF	[51]
^{4}He+^{238}U	23.00	2.02	10.04	0.001	0.024	0.024	FF	[54]
^{4}He+^{237}Np	21.12	0.64	9.39	2.391	0.810	0.877	EvR+FF	[55]
^{6}He+^{64}Zn	9.86	2.06	8.14	0	0.015	0.083	EvR	[56]
^{6}He+^{209}Bi	19.57	2.23	9.67	0	0.496	0.457	EvR	[57]
^{8}He+^{197}Au	19.61	1.95	11.41	0	0.196	0.331	EvR	[58]
^{6}Li+^{64}Ni	11.82	1.24	8.57	0	0.089	0.165	EvR	[59]
^{6}Li+^{64}Zn	12.68	1.63	8.75	0.161	0.392	1.802	EvR	[60]
^{6}Li+^{90}Zr	17.45	1.05	8.17	2.478	1.351	1.180	EvR	[61]
^{6}Li+^{144}Sm	25.02	1.66	7.70	0.145	0.931	4.811	EvR	[62]
^{6}Li+^{152}Sm	24.47	1.95	8.26	0	0.890	0.301	EvR	[63]
^{6}Li+^{159}Tb	24.27	2.01	8.08	0.189	0.433	0.353	EvR	[64]
^{6}Li+^{198}Pt	28.69	1.82	8.45	0.192	0.426	2.926	EvR	[65]
^{6}Li+^{197}Au	27.79	1.54	7.51	0	0.557	1.470	EvR	[66]
^{6}Li+^{209}Bi	29.87	1.84	8.71	0.104	0.168	0.451	EvR+FF	[67]
^{6}Li+^{232}Th	31.61	2.76	11.28	0.156	0.206	0.532	FF	[68]
^{6}Li+^{238}U	30.93	2.62	10.33	0.081	0.685	1.760	FF	[68]
^{7}Li+^{16}O	4.31	0.89	8.99	0.029	0.677	0.669	EvR	[69]
^{7}Li+^{28}Si	6.98	0.78	7.79	0	0.596	0.646	EvR	[70]
^{7}Li+^{59}Co	11.77	1.40	7.86	0	0.271	0.268	EvR	[71]
^{7}Li+^{64}Zn	12.60	1.26	9.09	0.181	0.644	4.213	EvR	[60]
^{7}Li+^{144}Sm	24.66	1.33	8.55	1.123	0.308	0.115	EvR	[72]
^{7}Li+^{152}Sm	24.23	1.96	8.61	0	1.176	0.555	EvR	[72]
^{7}Li+^{159}Tb	23.06	1.51	10.31	0.280	1.044	4.231	EvR	[73]
^{7}Li+^{198}Pt	28.06	1.66	9.52	0	0.108	0.363	EvR	[74]
^{7}Li+^{197}Au	28.79	1.80	10.32	0	0.019	0.044	EvR	[66]
^{7}Li+^{209}Bi	29.69	1.69	9.86	0.149	0.302	1.279	EvR+FF	[75]
^{7}Li+^{209}Bi	29.53	1.67	9.58	0.188	0.056	0.072	EvR+FF	[67]
^{7}Li+^{232}Th	31.12	2.12	11.00	0.120	0.366	6.620	FF	[68]
^{7}Li+^{235}U	31.59	2.13	12.23	0.337	0.354	0.136	FF	[76]
^{7}Li+^{238}U	31.20	2.12	11.02	0.138	2.202	6.573	FF	[68]
^{7}Be+^{58}Ni	16.27	2.07	9.33	0	0.005	0.040	EvR	[77]
^{7}Be+^{238}U	43.15	1.72	9.51	0.409	0.305	28.512	FF	[78]
^{9}Be+^{89}Y	21.00	1.25	8.34	0.111	3.127	1.782	EvR	[49]
^{9}Be+^{124}Sn	26.05	2.10	8.88	0	1.148	0.152	EvR	[79]
^{9}Be+^{144}Sm	31.45	1.56	10.03	0	0.145	0.711	EvR	[80]
^{9}Be+^{169}Tm	34.71	1.18	9.87	2.380	0.777	0.490	EvR	[81]
^{9}Be+^{181}Ta	35.95	2.01	9.09	0.466	0.471	0.193	EvR	[82]
^{9}Be+^{187}Re	37.01	2.08	9.92	0	0.346	0.439	EvR	[81]
^{9}Be+^{208}Pb	38.32	1.77	9.31	0	1.146	0.803	EvR+FF	[83]
^{9}Be+^{209}Bi	38.14	1.58	9.82	0.050	0.179	0.175	EvR	[84]
^{9}Be+^{209}Bi	38.15	1.56	10.01	0.107	0.199	0.466	EvR	[85]
^{9}Be+^{209}Bi	37.66	0.91	9.02	2.011	0.045	0.037	EvR	[86]
^{10}B+^{159}Tb	39.23	1.15	9.46	3.048	0.071	0.172	EvR	[87]
^{11}B+^{13}C	4.94	0.52	7.98	0.895	0.182	0.460	EvR	[88]
^{11}B+^{159}Tb	39.41	2.20	10.31	0	0.039	0.171	EvR	[87]
^{11}B+^{238}U	49.66	1.64	11.34	0.333	0.181	0.719	FF	[89]
^{11}B+^{237}Np	54.84	2.79	11.80	0	0.312	1.132	FF	[89]
^{12}C+^{9}Be	3.86	0.63	7.12	0	0.237	1.023	EvR	[90]
^{12}C+^{11}B	4.79	0.50	5.45	0.657	0.303	0.752	EvR	[91]
^{12}C+^{11}B	4.88	0.50	6.30	0.880	1.386	0.920	EvR	[92]
^{12}C+^{13}C	5.63	0.52	6.82	0.558	0.495	0.688	EvR	[92]
^{12}C+^{14}C	5.49	0.39	6.24	0	0.002	0.006	EvR	[93]
^{12}C+^{14}N	6.90	0.64	7.64	0.646	0.424	0.424	EvR	[92]
^{12}C+^{20}Ne	9.80	0.88	7.66	0.170	1.405	1.692	EvR	[94]
^{12}C+^{46}Ti	21.31	1.58	9.82	0.118	0.222	0.911	EvR	[95]
^{12}C+^{48}Ti	20.40	1.53	8.29	0	0.486	0.728	EvR	[95]
^{12}C+^{50}Ti	19.72	1.20	8.12	0.296	0.167	0.409	EvR	[95]
^{12}C+^{89}Y	32.17	1.50	10.50	0.202	0.256	0.830	EvR	[49]
^{12}C+^{92}Zr	31.82	1.25	9.13	0	3.264	13.703	EvR	[96]
^{12}C+^{144}Sm	46.83	1.54	11.63	0.127	0.501	1.100	EvR	[97]
^{12}C+^{152}Sm	47.22	2.09	11.20	2.101	0.043	0.024	EvR	[73]
^{12}C+^{154}Sm	44.54	0.84	9.40	1.831	0.144	0.302	EvR	[50]
^{12}C+^{181}Ta	52.43	2.07	10.66	0	0.211	0.216	EvR	[98]

(continued on next page)

Table A (*continued*).

$^{12}C+^{194}Pt$	54.91	1.52	10.34	0.127	1.115	0.363	EvR+FF	[99]
$^{12}C+^{198}Pt$	55.27	1.55	10.62	0.161	2.152	0.222	EvR+FF	[99]
$^{12}C+^{204}Pb$	55.99	1.04	11.23	0.190	0.482	2.494	EvR+FF	[100]
$^{12}C+^{208}Pb$	56.34	1.26	10.59	0	1.329	0.091	EvR+FF	[101]
$^{12}C+^{237}Np$	62.96	2.52	10.51	0	0.326	1.852	FF	[89]
$^{13}C+^{10}B$	4.94	0.63	7.67	0	0.124	0.190	EvR	[88]
$^{13}C+^{11}B$	5.02	0.54	8.44	0.864	0.200	0.212	EvR	[88]
$^{13}C+^{13}C$	5.98	0.64	8.08	0.335	34.259	0.956	EvR	[102]
$^{13}C+^{48}Ti$	20.50	2.45	8.64	0	0.074	0.190	EvR	[103]
$^{13}C+^{232}Th$	61.68	2.20	12.75	2.002	0.198	0.036	FF	[104]
$^{14}N+^{10}B$	5.72	0.65	7.79	0.153	0.180	1.105	EvR	[105]
$^{14}N+^{12}C$	6.90	0.64	7.64	0.648	0.430	0.430	EvR	[106]
$^{14}N+^{14}N$	7.55	0.74	6.10	0	0.024	0.042	EvR	[107]
$^{14}N+^{14}N$	8.25	0.81	8.12	0.181	2.372	1.327	EvR	[108]
$^{14}N+^{14}N$	8.23	0.80	8.11	0.196	1.537	1.370	EvR	[92]
$^{14}N+^{16}O$	9.23	0.83	8.70	0.199	0.221	0.228	EvR	[92]
$^{14}N+^{59}Co$	26.81	1.41	9.46	0.367	0.282	0.509	EvR	[109]
$^{14}N+^{232}Th$	70.99	2.03	12.13	1.933	0.185	0.163	FF	[110]
$^{15}N+^{54}Fe$	26.19	1.81	10.04	0	0.554	0.952	EvR	[111]
$^{15}N+^{209}Bi$	66.53	1.58	10.90	0	0.159	1.595	FF	[112]
$^{16}O+^{12}C$	7.72	0.67	7.81	0.543	4.989	1.782	EvR	[113]
$^{16}O+^{13}C$	7.80	0.80	7.29	0	0.344	0.590	EvR	[114]
$^{16}O+^{14}N$	9.16	0.82	8.25	0.176	0.259	0.268	EvR	[106]
$^{16}O+^{16}O$	10.34	0.92	8.50	0.146	0.253	0.250	EvR	[115]
$^{16}O+^{16}O$	10.32	0.95	9.09	0	0.229	0.638	EvR	[116]
$^{16}O+^{27}Al$	15.76	1.19	7.41	0	0.015	0.077	EvR	[117]
$^{16}O+^{46}Ti$	26.21	1.40	8.92	0.459	0.071	0.076	EvR	[118]
$^{16}O+^{50}Ti$	26.06	1.65	8.28	0.050	0.222	1.031	EvR	[109]
$^{16}O+^{50}Ti$	25.98	1.55	9.12	0.125	0.075	0.445	EvR	[118]
$^{16}O+^{54}Fe$	30.29	1.46	8.76	0.404	0.340	0.693	EvR	[111]
$^{16}O+^{56}Fe$	30.24	1.05	9.13	3.085	0.445	0.330	EvR	[111]
$^{16}O+^{58}Ni$	31.32	1.07	9.33	0.128	1.260	1.556	EvR	[119]
$^{16}O+^{62}Ni$	30.54	1.04	8.93	0.179	1.265	0.472	EvR	[119]
$^{16}O+^{63}Cu$	34.88	2.77	9.20	0	0.391	0.390	EvR	[120]
$^{16}O+^{63}Cu$	35.32	2.89	9.44	0	0.634	0.518	EvR	[121]
$^{16}O+^{63}Cu$	33.07	1.03	8.95	1.402	0.115	0.003	EvR	[122]
$^{16}O+^{65}Cu$	33.68	2.86	8.97	0	0.302	0.358	EvR	[120]
$^{16}O+^{64}Zn$	33.00	2.54	10.32	0	0.230	0.265	EvR	[123]
$^{16}O+^{70}Ge$	34.76	1.45	9.75	0	0.955	0.189	EvR	[124]
$^{16}O+^{72}Ge$	35.62	1.79	10.03	0	1.700	0.370	EvR	[124]
$^{16}O+^{73}Ge$	33.98	1.01	8.31	1.880	0.064	0.034	EvR	[124]
$^{16}O+^{74}Ge$	34.89	1.16	9.66	2.095	1.729	0.631	EvR	[124]
$^{16}O+^{76}Ge$	34.95	1.12	9.43	1.966	9.775	0.612	EvR	[125]
$^{16}O+^{76}Ge$	34.50	1.13	9.55	1.624	1.188	0.279	EvR	[124]
$^{16}O+^{92}Zr$	41.47	1.58	9.56	0	3.633	1.394	EvR	[96]
$^{16}O+^{112}Cd$	48.28	1.66	11.02	0	0.414	1.891	EvR	[126]
$^{16}O+^{112}Sn$	50.61	1.38	9.81	0.127	0.811	19.177	EvR	[127]
$^{16}O+^{116}Sn$	50.20	1.39	9.96	0.155	0.793	3.315	EvR	[127]
$^{16}O+^{144}Nd$	57.31	1.53	11.12	0	0.042	0.145	EvR	[128]
$^{16}O+^{150}Nd$	57.04	1.67	9.25	0	0.555	0.120	EvR	[73]
$^{16}O+^{144}Sm$	60.51	1.59	10.34	0	21.851	4.572	EvR	[129]
$^{16}O+^{147}Sm$	58.84	1.44	9.61	0	0.797	1.554	EvR	[130]
$^{16}O+^{148}Sm$	59.73	1.75	10.51	1.158	9.033	1.269	EvR	[129]
$^{16}O+^{148}Sm$	59.74	2.07	11.26	0	0.215	0.384	EvR	[130]
$^{16}O+^{148}Sm$	59.15	1.88	9.73	0	0.154	0.154	EvR	[131]
$^{16}O+^{149}Sm$	58.95	1.88	9.97	0	0.523	1.714	EvR	[130]
$^{16}O+^{150}Sm$	59.20	1.67	10.64	1.481	0.099	0.098	EvR	[131]
$^{16}O+^{152}Sm$	59.67	1.86	10.86	2.197	0.216	0.204	EvR	[131]
$^{16}O+^{154}Sm$	58.90	2.53	10.13	0	0.039	0.037	EvR	[131]
$^{16}O+^{154}Sm$	59.03	2.80	10.30	0	0.095	0.024	EvR	[132]
$^{16}O+^{154}Sm$	59.20	1.99	10.46	1.543	3.208	1.783	EvR	[129]
$^{16}O+^{154}Sm$	59.21	1.84	10.20	1.992	3.395	2.101	EvR	[133]
$^{16}O+^{166}Er$	63.66	1.48	10.29	2.643	0.673	1.126	EvR	[134]
$^{16}O+^{174}Yb$	66.52	2.59	10.93	0.119	0.639	1.329	EvR	[135]
$^{16}O+^{176}Yb$	66.79	2.94	9.75	0.100	1.420	4.830	EvR	[135]
$^{16}O+^{186}W$	68.31	2.29	10.44	0	6.333	1.323	EvR+FF	[136]
$^{16}O+^{186}W$	68.18	2.13	10.38	0.106	0.383	1.874	EvR+FF	[137]
$^{16}O+^{194}Pt$	72.60	2.18	11.73	0.003	0.028	0.047	EvR+FF	[138,139]
$^{16}O+^{208}Pb$	73.79	1.20	10.62	1.877	29.330	0.089	EvR+FF	[33]
$^{16}O+^{208}Pb$	74.13	1.23	10.59	2.135	0.097	0.151	EvR+FF	[112]
$^{16}O+^{209}Bi$	75.03	1.21	10.75	2.245	0.088	0.138	FF	[112]
$^{16}O+^{209}Bi$	77.17	2.43	10.11	0.219	1.923	2.397	FF	[140]
$^{17}O+^{12}C$	7.66	0.70	7.27	0.208	0.111	0.065	EvR	[141]
$^{17}O+^{12}C$	9.50	0.83	11.51	3.671	1.253	2.932	EvR	[142]
$^{17}O+^{13}C$	7.88	0.63	6.81	0.080	0.275	0.432	EvR	[142]

(*continued on next page*)

Table A (*continued*).

^{17}O+^{16}O	10.08	0.93	9.11	0.143	0.628	11.320	EvR	[116]
^{17}O+^{144}Sm	60.25	1.86	10.42	0	5.928	4.610	EvR	[129]
^{18}O+^{9}Be	4.96	0.49	6.57	0.858	0.090	1.765	EvR	[143]
^{18}O+^{12}C	7.43	0.35	7.34	2.401	0.052	0.028	EvR	[141]
^{18}O+^{12}C	7.71	0.87	7.42	0	0.608	0.729	EvR	[144]
^{18}O+^{16}O	9.90	0.85	8.07	0.153	0.419	0.769	EvR	[116]
^{18}O+^{44}Ca	22.44	1.37	8.35	0.027	0.230	0.643	EvR	[95]
^{18}O+^{58}Ni	31.68	2.85	8.02	0	2.540	0.995	EvR	[145]
^{18}O+^{60}Ni	33.77	2.72	10.70	0	1.474	1.493	EvR	[146]
^{18}O+^{64}Ni	33.29	2.36	9.77	0	0.456	0.488	EvR	[146]
^{18}O+^{63}Cu	34.32	2.30	10.09	0.513	0.229	0.186	EvR	[120]
^{18}O+^{74}Ge	34.31	1.09	9.23	2.076	32.807	0.795	EvR	[125]
^{18}O+^{148}Nd	58.21	2.95	9.13	0	0.088	0.101	EvR	[73]
^{18}O+^{208}Pb	74.14	1.33	10.79	2.562	0.175	0.290	FF	[112]
^{19}F+^{54}Fe	33.87	3.14	9.50	0	0.334	0.564	EvR	[111]
^{19}F+^{56}Fe	33.00	2.73	9.10	0	0.611	0.852	EvR	[111]
^{19}F+^{93}Nb	47.66	2.31	9.98	0	0.965	0.217	EvR	[147]
^{19}F+^{181}Ta	76.22	2.90	10.96	0.954	0.149	0.031	EvR+FF	[148]
^{19}F+^{188}Os	78.21	2.96	10.34	0	0.208	0.259	EvR+FF	[149]
^{19}F+^{192}Os	78.80	2.11	10.31	3.142	0.028	0.028	EvR+FF	[149]
^{19}F+^{208}Pb	82.48	2.28	10.97	0.516	12.345	0.161	EvR+FF	[150]
^{19}F+^{208}Pb	83.47	2.71	11.22	0.275	0.211	0.294	FF	[151]
^{19}F+^{208}Pb	83.04	2.57	12.87	0.066	0.772	3.277	FF	[152]
^{19}F+^{209}Bi	83.96	2.60	10.84	0	0.722	0.337	FF	[153]
^{19}F+^{232}Th	87.85	3.90	9.91	0	0.698	0.732	FF	[154]
^{19}F+^{232}Th	89.94	4.23	12.01	0	0.034	0.071	FF	[155]
^{19}F+^{232}Th	90.28	4.61	13.51	0.373	1.815	6.393	FF	[156]
^{20}Ne+^{208}Pb	94.52	2.16	11.22	2.121	0.600	1.025	FF	[157]
^{20}Ne+^{238}U	102.82	5.08	12.52	0	0.703	0.933	FF	[158]
^{23}Na+^{48}Ti	33.45	0.86	9.30	3.361	0.199	0.365	EvR	[159]
^{23}Na+^{206}Pb	99.46	2.74	11.59	0.002	0.002	0.006	FF	[159]
^{24}Mg+^{24}Mg	22.07	1.09	8.57	1.437	1.341	0.194	EvR	[160]
^{24}Mg+^{26}Mg	20.89	1.24	8.35	0	0.376	0.047	EvR	[160]
^{24}Mg+^{30}Si	24.10	1.06	8.07	0.107	0.260	1.108	EvR	[161]
^{26}Mg+^{248}Cm	128.60	5.16	14.09	0.313	0.043	1.212	FF	[162]
^{27}Al+^{45}Sc	37.86	1.33	7.70	0.237	0.102	1.927	EvR	[163]
^{27}Al+^{70}Ge	54.15	1.76	9.08	0	1.856	0.719	EvR	[164]
^{27}Al+^{72}Ge	54.00	1.61	9.02	0.238	1.700	0.750	EvR	[164]
^{27}Al+^{73}Ge	54.12	1.60	8.79	1.254	0.485	0.363	EvR	[164]
^{27}Al+^{74}Ge	53.15	1.20	8.14	1.475	0.846	0.689	EvR	[164]
^{27}Al+^{76}Ge	53.17	1.33	8.87	1.220	1.028	0.428	EvR	[164]
^{29}Al+^{197}Au	111.09	2.96	11.00	0	0.090	0.528	FF	[165]
^{28}Si+^{24}Mg	24.51	1.09	8.13	0.082	1.035	15.515	EvR	[166]
^{28}Si+^{24}Mg	24.64	0.91	8.10	1.318	1.536	0.160	EvR	[160]
^{28}Si+^{26}Mg	24.91	1.10	8.47	0.110	1.834	1.834	EvR	[166]
^{28}Si+^{28}Si	29.03	1.63	8.26	0	2.384	0.919	EvR	[160]
^{28}Si+^{28}Si	29.53	1.41	9.12	0.207	0.805	25.466	EvR	[167]
^{28}Si+^{29}Si	28.53	1.42	8.24	0	2.245	1.188	EvR	[160]
^{28}Si+^{30}Si	28.22	1.41	8.41	0	1.645	0.270	EvR	[160]
^{28}Si+^{30}Si	28.73	1.75	8.18	0	0.158	0.441	EvR	[95]
^{28}Si+^{30}Si	28.19	1.13	8.02	0.120	1.054	1.217	EvR	[168]
^{28}Si+^{58}Ni	53.92	1.52	9.01	0.188	3.051	8.115	EvR	[169]
^{28}Si+^{62}Ni	51.33	1.22	7.86	0	0.254	2.776	EvR	[170]
^{28}Si+^{64}Ni	51.33	0.99	8.51	2.686	0.167	0.910	EvR	[170]
^{28}Si+^{64}Ni	50.37	1.30	7.23	0.131	0.328	1.643	EvR	[171]
^{28}Si+^{64}Ni	50.72	1.23	7.18	0	0.100	0.584	EvR	[172]
^{28}Si+^{68}Zn	53.43	1.40	7.47	0	4.352	3.577	EvR	[173]
^{28}Si+^{68}Zn	53.42	1.44	7.67	0	0.350	2.250	EvR	[174]
^{28}Si+^{90}Zr	72.36	2.17	10.24	0.110	0.795	1.751	EvR	[175]
^{28}Si+^{92}Zr	70.23	2.47	9.63	0	5.736	0.540	EvR	[96]
^{28}Si+^{94}Zr	69.70	1.94	8.25	0.208	1.532	5.135	EvR	[175]
^{28}Si+^{96}Zr	70.00	1.81	9.75	2.990	0.501	1.160	EvR	[176]
^{28}Si+^{93}Nb	73.52	1.63	10.45	2.972	0.176	0.733	EvR	[177]
^{28}Si+^{94}Mo	74.20	1.26	8.03	2.142	2.164	213.559	EvR	[178]
^{28}Si+^{94}Mo	75.35	1.75	8.89	1.487	0.239	1.190	EvR	[179]
^{28}Si+^{144}Nd	101.95	2.64	11.94	2.348	0.421	0.244	EvR	[172]
^{28}Si+^{154}Sm	101.11	4.85	10.58	0	1.434	2.274	EvR	[180]
^{28}Si+^{164}Er	107.01	3.50	11.66	2.516	0.038	0.051	EvR+FF	[181]
^{28}Si+^{170}Er	104.15	2.69	11.31	3.969	0.032	0.061	EvR+FF	[181]
^{28}Si+^{178}Hf	114.59	2.98	10.75	2.453	7.061	0.197	EvR+FF	[182]
^{28}Si+^{198}Pt	121.64	2.54	10.28	2.171	0.276	0.618	FF	[183]
^{28}Si+^{208}Pb	126.74	2.15	10.88	3.212	0.147	0.150	FF	[184]
^{29}Si+^{178}Hf	114.73	4.36	11.15	0	11.560	2.254	EvR+FF	[182]
^{30}Si+^{24}Mg	23.98	1.01	8.07	0	0.326	0.293	EvR	[166]
^{30}Si+^{26}Mg	24.87	1.14	9.51	0.140	2.310	4.394	EvR	[166]

(*continued on next page*)

Table A (*continued*).

^{30}Si+^{30}Si	28.10	0.91	8.60	0	0.763	1.862	EvR	[95]
^{30}Si+^{58}Ni	52.74	1.44	8.70	0.277	0.220	1.676	EvR	[170]
^{30}Si+^{62}Ni	51.94	1.42	9.57	0.180	0.552	7.554	EvR	[170]
^{30}Si+^{64}Ni	51.29	1.31	9.45	0.190	0.404	0.902	EvR	[170]
^{30}Si+^{170}Er	109.34	3.40	11.61	2.020	0.087	0.180	EvR+FF	[148]
^{30}Si+^{238}U	137.63	5.38	13.12	0.271	0.228	5.523	FF	[185]
^{30}Si+^{238}U	137.69	4.68	11.07	0	0.285	6.054	FF	[186]
^{31}P+^{175}Lu	120.53	4.75	10.98	0	2.505	0.171	EvR+FF	[182]
^{32}S+^{12}C	15.14	1.07	8.30	0	0.291	1.010	EvR	[187]
^{32}S+^{13}C	15.78	1.29	9.55	0.077	0.276	0.743	EvR	[187]
^{32}S+^{24}Mg	27.84	1.12	8.71	0.489	0.118	0.178	EvR	[188]
^{32}S+^{25}Mg	27.09	1.11	8.31	0	0.256	0.378	EvR	[188]
^{32}S+^{26}Mg	27.05	1.19	8.47	0	0.305	0.820	EvR	[188]
^{32}S+^{27}Al	29.70	1.17	8.78	0	0.612	1.004	EvR	[188]
^{32}S+^{48}Ca	42.57	1.49	8.16	0.182	0.114	6.221	EvR	[189]
^{32}S+^{58}Ni	58.47	0.89	8.21	1.724	1.002	2.401	EvR	[190]
^{32}S+^{58}Ni	59.64	1.32	8.49	0.114	0.264	1.688	EvR	[170]
^{32}S+^{58}Ni	59.60	1.29	8.38	0.156	0.672	2.871	EvR	[191]
^{32}S+^{64}Ni	56.74	1.03	8.38	2.005	0.314	0.154	EvR	[190]
^{32}S+^{64}Ni	58.94	1.73	10.21	2.964	1.238	0.704	EvR	[173]
^{32}S+^{64}Ni	59.40	2.99	11.03	0	0.239	1.661	EvR	[174]
^{32}S+^{64}Ni	57.44	1.51	8.32	0.154	0.361	2.129	EvR	[191]
^{32}S+^{64}Ni	57.41	1.51	8.33	0.156	0.321	2.559	EvR	[170]
^{32}S+^{89}Y	76.94	1.22	9.63	2.132	9.856	2.061	EvR	[192]
^{32}S+^{90}Zr	79.37	1.68	10.40	2.180	44.555	4.001	EvR	[37]
^{32}S+^{94}Zr	78.97	2.53	10.80	1.692	41.002	2.852	EvR	[193]
^{32}S+^{96}Zr	78.20	2.31	10.11	1.949	42.939	1.809	EvR	[37]
^{32}S+^{94}Mo	83.16	2.35	10.73	0	1.253	56.894	EvR	[194]
^{32}S+^{98}Mo	82.16	1.89	9.20	2.777	5.571	13.037	EvR	[194]
^{32}S+^{100}Mo	83.29	2.57	10.18	1.925	2.959	2.484	EvR	[194]
^{32}S+^{100}Ru	84.05	1.88	8.32	0.182	0.218	8.962	EvR	[194]
^{32}S+^{101}Ru	84.77	2.61	8.51	0	0.279	0.902	EvR	[194]
^{32}S+^{102}Ru	84.04	2.31	8.59	0	0.615	2.061	EvR	[194]
^{32}S+^{104}Ru	83.31	2.58	8.38	0	0.075	0.449	EvR	[194]
^{32}S+^{103}Rh	85.24	1.71	7.33	1.083	1.754	6.753	EvR	[194]
^{32}S+^{105}Pd	86.80	2.13	7.35	0	0.046	0.230	EvR	[194]
^{32}S+^{106}Pd	86.00	1.80	7.28	0	0.304	2.938	EvR	[194]
^{32}S+^{108}Pd	85.77	2.05	7.69	0	0.199	3.589	EvR	[194]
^{32}S+^{110}Pd	87.01	2.15	8.61	1.395	11.141	0.390	EvR	[38]
^{32}S+^{110}Pd	87.82	2.18	8.59	1.863	0.275	0.583	EvR	[194]
^{32}S+^{112}Sn	94.98	1.73	8.93	0.965	0.117	0.598	EvR	[127]
^{32}S+^{120}Sn	94.13	1.89	9.65	1.738	0.255	0.331	EvR	[127]
^{32}S+^{138}Ba	107.55	3.14	10.36	1.241	4.382	3.078	EvR+FF	[195]
^{32}S+^{154}Sm	112.78	3.64	8.91	1.133	0.220	0.403	EvR+FF	[196]
^{32}S+^{182}W	131.10	2.39	9.89	2.575	0.526	2.395	FF	[197]
^{32}S+^{184}W	127.12	2.91	9.24	0.193	0.153	0.224	EvR+FF	[198,199]
^{33}S+^{91}Zr	78.63	1.75	9.52	0	0.201	0.976	EvR	[200]
^{33}S+^{92}Zr	78.78	1.55	10.08	2.218	0.269	1.992	EvR	[200]
^{34}S+^{24}Mg	27.50	1.12	9.31	0.129	0.616	7.702	EvR	[188]
^{34}S+^{26}Mg	26.93	1.00	9.00	0	0.675	1.539	EvR	[188]
^{34}S+^{58}Ni	58.60	1.27	7.78	0	0.058	0.385	EvR	[170]
^{34}S+^{64}Ni	56.42	1.37	8.52	0	0.412	0.250	EvR	[190]
^{34}S+^{64}Ni	56.99	1.29	8.81	0	0.090	0.490	EvR	[170]
^{34}S+^{89}Y	76.10	1.42	9.67	0	11.382	2.220	EvR	[192]
^{34}S+^{168}Er	121.60	2.96	10.46	2.055	2.564	0.123	EvR+FF	[34]
^{34}S+^{168}Er	121.44	2.88	10.36	2.109	0.065	0.045	EvR+FF	[201]
^{34}S+^{168}Er	123.61	3.29	10.64	1.883	2.333	0.346	FF	[34]
^{34}S+^{204}Pb	142.41	2.65	9.43	0	0.078	5.638	FF	[202]
^{34}S+^{206}Pb	140.84	1.97	8.80	0	0.205	13.544	FF	[202]
^{34}S+^{208}Pb	141.30	1.59	9.56	2.378	0.437	10.072	FF	[202]
^{34}S+^{238}U	153.29	4.77	8.95	0	0.074	1.046	FF	[203]
^{36}S+^{48}Ca	42.44	1.22	10.39	0.232	0.603	2.775	EvR	[204]
^{36}S+^{48}Ca	42.15	1.09	11.13	0.238	1.091	21.585	EvR	[205]
^{36}S+^{58}Ni	58.30	1.42	7.58	0.171	0.105	0.644	EvR	[170]
^{36}S+^{58}Ni	58.34	1.42	7.91	0.184	0.162	0.834	EvR	[191]
^{36}S+^{64}Ni	57.04	1.17	8.88	0.153	0.415	1.875	EvR	[191]
^{36}S+^{64}Ni	56.87	1.14	8.83	0.137	0.157	1.386	EvR	[170]
^{36}S+^{64}Ni	56.25	1.19	9.79	0.121	5.629	2.783	EvR	[206]
^{36}S+^{90}Zr	77.22	1.36	11.14	0	3.920	1.672	EvR	[207]
^{36}S+^{96}Zr	75.35	1.00	11.46	3.648	3.854	4.935	EvR	[207]
^{36}S+^{92}Mo	84.87	2.04	13.87	3.928	0.499	9.453	EvR	[194]
^{36}S+^{94}Mo	80.82	1.91	10.25	0	0.665	7.829	EvR	[194]
^{36}S+^{96}Mo	79.83	1.14	8.41	2.051	2.374	8.993	EvR	[194]
^{36}S+^{98}Mo	78.61	0.83	8.68	2.667	0.810	1.136	EvR	[194]
^{36}S+^{100}Mo	78.92	1.08	10.02	2.689	0.492	1.379	EvR	[194]

(continued on next page)

Table A (*continued*).

^{36}S+^{100}Ru	82.93	1.24	8.45	1.542	0.731	14.787	EvR	[194]
^{36}S+^{101}Ru	82.79	1.64	9.75	0	0.122	0.346	EvR	[194]
^{36}S+^{102}Ru	81.97	1.41	8.42	0.021	7.317	3.355	EvR	[194]
^{36}S+^{104}Ru	83.18	1.50	10.54	2.216	2.312	6.163	EvR	[194]
^{36}S+^{106}Pd	87.76	1.48	11.02	3.750	0.955	4.883	EvR	[194]
^{36}S+^{108}Pd	87.49	1.55	10.41	3.395	0.071	2.187	EvR	[194]
^{36}S+^{110}Pd	86.08	1.52	8.57	1.819	7.026	0.932	EvR	[38]
^{36}S+^{110}Pd	84.74	1.53	7.96	0.161	1.484	19.173	EvR	[194]
^{36}S+^{204}Pb	141.08	1.01	9.60	3.362	0.203	3.384	FF	[202]
^{36}S+^{206}Pb	139.98	1.38	8.97	0	0.463	9.838	FF	[202]
^{36}S+^{208}Pb	139.90	1.36	9.92	0	0.282	6.264	FF	[202]
^{36}S+^{238}U	154.81	4.19	12.26	0.904	0.424	2.015	FF	[162]
^{35}Cl+^{24}Mg	30.22	1.65	9.84	0.192	1.597	1.928	EvR	[208]
^{35}Cl+^{25}Mg	30.08	1.85	9.31	0	0.980	1.047	EvR	[208]
^{35}Cl+^{26}Mg	29.47	1.93	8.29	0	0.378	0.370	EvR	[208]
^{35}Cl+^{27}Al	30.55	0.76	8.26	0	0.234	0.110	EvR	[209]
^{35}Cl+^{51}V	51.66	1.59	10.38	0.012	0.153	0.190	EvR	[210]
^{35}Cl+^{58}Ni	61.32	1.40	9.00	0	0.907	1.373	EvR	[209]
^{35}Cl+^{60}Ni	61.03	2.12	9.27	0	0.511	1.583	EvR	[209]
^{35}Cl+^{62}Ni	60.59	1.53	9.48	1.615	0.214	0.107	EvR+FF	[209]
^{35}Cl+^{62}Ni	60.73	1.57	9.65	1.850	0.190	0.143	EvR	[211]
^{35}Cl+^{62}Ni	60.71	1.69	9.59	1.318	0.089	0.067	EvR	[209]
^{35}Cl+^{64}Ni	60.30	2.26	9.67	0	0.373	0.388	EvR	[209]
^{35}Cl+^{92}Zr	82.50	2.33	9.74	0	2.757	1.044	EvR	[96]
^{35}Cl+^{130}Te	102.37	2.71	11.67	0	0.191	0.281	EvR+FF	[212]
^{37}Cl+^{24}Mg	29.39	1.98	8.54	0	0.467	0.493	EvR	[208]
^{37}Cl+^{25}Mg	28.86	0.91	8.34	1.775	2.435	4.320	EvR	[208]
^{37}Cl+^{26}Mg	28.61	0.87	7.59	1.779	0.452	0.441	EvR	[208]
^{37}Cl+^{59}Co	58.36	1.48	8.74	0	1.252	0.701	EvR	[173]
^{37}Cl+^{70}Ge	66.97	1.68	8.31	0	0.741	0.600	EvR	[213]
^{37}Cl+^{72}Ge	67.01	1.60	8.90	0	1.121	0.300	EvR	[213]
^{37}Cl+^{73}Ge	67.45	2.41	8.37	0	0.877	0.327	EvR	[213]
^{37}Cl+^{74}Ge	68.04	2.52	9.75	0	0.361	0.175	EvR	[213]
^{37}Cl+^{76}Ge	68.13	1.62	10.11	2.461	0.405	0.122	EvR	[213]
^{37}Cl+^{98}Mo	84.98	1.93	8.38	0	0.127	0.366	EvR	[214]
^{40}Ar+^{110}Pd	97.26	4.08	11.04	0	0.457	1.256	EvR	[132]
^{40}Ar+^{112}Sn	104.77	1.86	9.43	1.910	0.776	1.075	EvR+FF	[215]
^{40}Ar+^{116}Sn	104.89	1.99	9.65	2.267	0.371	0.194	EvR+FF	[215]
^{40}Ar+^{122}Sn	104.55	2.13	10.38	2.020	1.832	2.154	EvR+FF	[215]
^{40}Ar+^{144}Sm	125.75	2.01	9.24	1.674	2.289	2.525	EvR+FF	[215]
^{40}Ar+^{144}Sm	126.73	2.20	9.61	1.539	0.602	2.438	EvR	[216]
^{40}Ar+^{148}Sm	127.50	3.07	10.42	1.902	2.628	6.590	EvR+FF	[215]
^{40}Ar+^{148}Sm	127.36	3.01	10.11	2.778	0.766	3.722	EvR	[216]
^{40}Ar+^{154}Sm	125.41	3.66	9.71	1.981	8.926	16.085	EvR+FF	[215]
^{40}Ar+^{154}Sm	126.04	5.14	12.49	0	0.496	1.687	EvR	[216]
^{40}Ar+^{176}Hf	146.00	7.23	10.89	0	0.887	0.244	FF	[217]
^{40}Ar+^{179}Hf	144.96	7.24	10.86	0	0.595	0.146	FF	[217]
^{40}Ar+^{208}Pb	158.75	3.86	10.56	0	4.271	1.273	FF	[217]
^{40}Ca+^{40}Ca	53.32	1.37	9.93	0.137	1.689	8.400	EvR	[218]
^{40}Ca+^{40}Ca	53.51	1.31	10.15	0.165	0.636	7.953	EvR	[219]
^{40}Ca+^{44}Ca	52.08	1.16	8.75	1.658	0.281	4.082	EvR	[218]
^{40}Ca+^{48}Ca	51.28	1.47	7.86	0	0.328	2.327	EvR	[218]
^{40}Ca+^{48}Ca	51.87	1.37	8.24	0.813	4.253	2.502	EvR	[220]
^{40}Ca+^{48}Ca	51.68	1.67	11.29	0.043	8.322	1.094	EvR	[221]
^{40}Ca+^{46}Ti	57.21	1.41	9.37	0	0.128	0.459	EvR	[222]
^{40}Ca+^{48}Ti	56.97	1.45	9.20	0	0.052	0.250	EvR	[222]
^{40}Ca+^{50}Ti	57.00	1.62	9.03	0	0.024	0.093	EvR	[222]
^{40}Ca+^{58}Ni	71.71	1.90	8.87	0	0.458	1.120	EvR	[223]
^{40}Ca+^{58}Ni	71.15	1.30	8.60	0	0.342	0.890	EvR	[224]
^{40}Ca+^{60}Ni	70.93	1.99	9.46	0	0.068	0.358	EvR	[223]
^{40}Ca+^{62}Ni	70.66	2.32	9.39	0	0.257	0.472	EvR+FF	[223]
^{40}Ca+^{62}Ni	70.80	2.39	9.52	0	0.341	0.668	EvR	[223]
^{40}Ca+^{64}Ni	69.44	1.39	8.68	1.412	0.808	6.110	EvR	[224]
^{40}Ca+^{90}Zr	96.18	1.58	10.00	0	5.326	0.226	EvR	[26]
^{40}Ca+^{90}Zr	96.40	1.54	9.97	0	0.304	0.218	EvR	[225]
^{40}Ca+^{94}Zr	94.95	2.60	9.96	0.394	0.601	0.197	EvR	[226]
^{40}Ca+^{96}Zr	94.09	2.16	9.62	1.443	3.419	0.115	EvR	[26]
^{40}Ca+^{96}Zr	94.32	2.17	9.60	1.411	0.079	0.063	EvR	[225]
^{40}Ca+^{96}Zr	95.05	2.28	10.29	2.304	0.108	0.621	EvR	[227]
^{40}Ca+^{124}Sn	113.22	2.19	9.62	0.869	2.543	0.248	EvR	[228]
^{40}Ca+^{124}Sn	113.34	2.26	9.56	0.792	1.399	0.119	EvR	[229]
^{40}Ca+^{192}Os	166.75	4.69	10.24	0.185	0.368	2.358	FF	[230]
^{40}Ca+^{194}Pt	171.46	3.31	9.71	1.473	0.386	0.889	FF	[230]
^{40}Ca+^{197}Au	174.59	6.84	10.61	0.179	3.159	1.645	FF	[231]
^{40}Ca+^{208}Pb	176.68	3.91	9.96	2.503	5.646	0.098	FF	[231]

(*continued on next page*)

Table A (*continued*).

^{40}Ca+^{238}U	192.86	5.60	8.57	0	0.182	0.464	FF	[232]
^{48}Ca+^{48}Ca	51.51	1.10	10.43	0.202	2.655	36.945	EvR	[233]
^{48}Ca+^{48}Ca	51.04	0.88	10.68	0.814	3.075	0.798	EvR	[221]
^{48}Ca+^{90}Zr	94.70	1.78	9.86	0	5.126	2.074	EvR	[234]
^{48}Ca+^{96}Zr	93.43	1.31	10.06	3.871	7.090	0.737	EvR	[234]
^{48}Ca+^{154}Sm	140.22	4.16	10.63	1.811	1.856	3.485	EvR+FF	[235]
^{48}Ca+^{154}Sm	138.49	3.44	10.65	2.228	2.308	3.587	EvR+FF	[236]
^{48}Ca+^{208}Pb	175.48	2.89	12.53	0	2.821	18.852	FF	[237]
^{48}Ca+^{238}U	193.27	4.62	11.55	0.204	0.114	0.865	FF	[232]
^{45}Sc+^{51}V	61.82	1.40	8.74	1.902	0.130	0.374	EvR	[173]
^{46}Ti+^{46}Ti	63.09	1.55	10.74	2.091	5.638	0.937	EvR	[238]
^{46}Ti+^{64}Ni	77.05	2.03	9.58	1.464	1.147	0.442	EvR	[147]
^{46}Ti+^{90}Zr	106.23	2.37	10.45	1.007	0.343	0.237	EvR	[15]
^{46}Ti+^{93}Nb	108.70	3.61	10.78	0	0.404	0.132	EvR	[15]
^{48}Ti+^{58}Fe	71.50	1.43	8.58	1.425	0.226	2.531	EvR	[239]
^{48}Ti+^{58}Ni	78.88	2.24	9.85	0.176	1.667	0.582	EvR	[240]
^{48}Ti+^{60}Ni	77.39	1.80	9.89	0.166	1.683	0.616	EvR	[240]
^{48}Ti+^{64}Ni	77.99	1.62	11.65	3.759	6.520	2.380	EvR	[240]
^{48}Ti+^{122}Sn	126.45	2.40	9.43	1.866	2.875	0.952	EvR+FF	[195]
^{50}Ti+^{60}Ni	77.27	1.99	9.87	0.128	2.075	1.297	EvR	[147]
^{50}Ti+^{90}Zr	104.29	1.37	10.05	1.753	0.464	0.130	EvR	[15]
^{50}Ti+^{93}Nb	106.76	1.81	10.16	1.788	0.438	0.580	EvR	[15]
^{58}Ni+^{54}Fe	91.67	1.25	9.02	2.571	0.413	2.641	EvR	[241]
^{58}Ni+^{54}Fe	91.90	1.33	9.41	2.414	5.177	2.836	EvR	[40]
^{58}Ni+^{54}Fe	91.78	1.30	8.94	2.330	0.330	2.227	EvR	[239]
^{58}Ni+^{58}Ni	99.19	1.47	8.09	2.535	1.094	3.762	EvR	[242]
^{58}Ni+^{60}Ni	97.99	1.68	8.34	2.356	6.947	1.402	EvR	[41]
^{58}Ni+^{64}Ni	95.43	1.98	8.49	0.397	0.392	1.773	EvR	[178]
^{58}Ni+^{64}Ni	96.67	1.97	8.45	2.487	0.750	2.661	EvR	[243]
^{58}Ni+^{74}Ge	108.30	2.62	7.94	1.336	0.658	2.104	EvR	[244]
^{58}Ni+^{90}Zr	133.74	2.18	7.76	1.765	0.031	0.177	EvR	[245]
^{58}Ni+^{92}Mo	138.89	2.55	8.33	0	0.109	0.300	EvR	[246]
^{58}Ni+^{100}Mo	139.59	3.50	10.09	2.490	0.084	0.235	EvR	[246]
^{58}Ni+^{112}Sn	159.52	4.67	7.53	0.613	0.067	0.128	EvR+FF	[247]
^{58}Ni+^{112}Sn	165.50	7.01	7.82	0.466	0.035	0.138	EvR+FF	[248]
^{58}Ni+^{114}Sn	162.31	6.13	7.33	0	0.866	3.934	EvR+FF	[248]
^{58}Ni+^{116}Sn	166.79	5.35	9.12	2.330	0.133	0.703	EvR+FF	[248]
^{58}Ni+^{118}Sn	163.22	3.19	8.15	2.835	0.038	0.134	EvR+FF	[248]
^{58}Ni+^{120}Sn	163.71	3.91	8.71	2.083	0.044	0.221	EvR+FF	[248]
^{58}Ni+^{124}Sn	162.02	5.63	8.93	0	0.325	1.596	EvR+FF	[248]
^{58}Ni+^{124}Sn	157.46	3.99	9.44	0	0.001	0.001	EvR+FF	[247]
^{58}Ni+^{124}Sn	158.28	3.09	9.68	1.235	0.498	4.938	EvR	[249]
^{60}Ni+^{89}Y	129.25	1.58	7.45	1.597	0.529	4.631	EvR	[250]
^{60}Ni+^{100}Mo	136.03	2.97	8.33	1.627	0.532	1.381	EvR	[251]
^{64}Ni+^{58}Ni	96.48	3.03	7.91	0	0.037	0.037	EvR	[244]
^{64}Ni+^{64}Ni	94.99	1.47	10.16	1.699	0.515	2.542	EvR	[178]
^{64}Ni+^{64}Ni	93.74	1.30	8.57	2.605	0.419	1.110	EvR	[244]
^{64}Ni+^{64}Ni	94.45	1.23	9.69	1.908	1.919	7.259	EvR	[179]
^{64}Ni+^{64}Ni	92.43	1.32	8.40	0.217	0.333	1.269	EvR	[252]
^{64}Ni+^{74}Ge	104.61	1.79	7.50	1.553	0.856	2.461	EvR	[244]
^{64}Ni+^{92}Zr	131.72	3.09	7.39	0.167	0.169	0.605	EvR	[253]
^{64}Ni+^{96}Zr	128.96	2.39	8.09	1.763	0.173	0.444	EvR	[253]
^{64}Ni+^{92}Mo	135.86	3.04	9.41	0	0.400	1.219	EvR	[246]
^{64}Ni+^{100}Mo	134.56	3.34	7.78	0.793	0.246	0.979	EvR	[246]
^{64}Ni+^{112}Sn	157.61	2.69	8.64	3.062	0.195	0.913	EvR+FF	[248]
^{64}Ni+^{114}Sn	158.85	4.08	9.37	0	0.000	0.000	EvR+FF	[248]
^{64}Ni+^{116}Sn	158.47	3.92	10.02	0	0.180	0.843	EvR+FF	[248]
^{64}Ni+^{118}Sn	157.41	4.31	9.36	0	0.481	0.757	EvR+FF	[254,255]
^{64}Ni+^{120}Sn	156.44	3.54	9.33	0	0.036	0.178	EvR+FF	[248]
^{64}Ni+^{122}Sn	155.99	2.26	9.41	3.600	0.018	0.083	EvR+FF	[248]
^{64}Ni+^{124}Sn	154.87	2.85	9.60	0	0.034	0.172	EvR+FF	[248]
^{74}Ge+^{74}Ge	122.45	3.47	8.21	1.515	0.585	1.154	EvR	[256]
^{81}Br+^{94}Zr	156.41	4.39	7.58	0	0.011	0.044	EvR	[257]
^{86}Kr+^{70}Ge	133.71	2.88	9.10	1.737	7.133	7.799	EvR	[258]
^{86}Kr+^{76}Ge	131.48	2.43	9.27	2.101	1.960	0.587	EvR	[258]
^{124}Sn+^{40}Ca	113.18	2.38	9.66	0.889	0.582	0.362	EvR	[259]
^{124}Sn+^{48}Ca	113.69	1.80	9.99	1.273	2.509	1.601	EvR	[259]
^{132}Sn+^{40}Ca	115.24	2.98	11.06	1.241	1.235	2.956	EvR	[259]
^{132}Sn+^{58}Ni	159.45	4.26	11.32	0.708	0.152	0.199	EvR+FF	[260]
^{132}Sn+^{64}Ni	151.09	5.83	8.23	0	0.221	0.418	EvR	[261]
^{132}Sn+^{64}Ni	157.61	3.08	11.97	3.865	0.090	0.198	EvR+FF	[262]
^{134}Te+^{40}Ca	116.79	2.28	8.79	0	0.531	0.426	EvR	[263]
^{134}Te+^{64}Ni	164.21	2.67	9.22	1.816	0.317	0.455	EvR	[264]
^{208}Pb+^{50}Ti	194.55	2.22	7.83	2.791	0.797	0.675	FF	[48]

Declaration of competing interest

The authors declare the following financial interests/personal relationships which may be considered as potential competing interests: Ning Wang reports financial support was provided by National Natural Science Foundation of China. Min Liu reports financial support was provided by National Natural Science Foundation of China. Ning Wang reports financial support was provided by Natural Science Foundation of Guangxi. Junlong Tian reports financial support was provided by Natural Science Foundation of Guangxi.

Data availability

Data available at http://www.imqmd.com/fusion/MSW_barrier.txt.

Acknowledgments

This work was supported by the National Natural Science Foundation of China[http://dx.doi.org/10.13039/501100001809] (Grant No. 12265006, U1867212), the Guangxi Natural Science Foundation (Grant NO. 2023GXNSFDA026005, 2017GXNSFGA198001) and the Middle-aged and Young Teachers' Basic Ability Promotion Project of Guangxi (CN) (Grant No. 2019KY0061). The authors would like to thank Huiming Jia and Li Ou for helpful discussions.

Appendix

See Table A.

References

[1] S. Hofmann, G. Münzenberg, Rev. Modern Phys. 72 (2000) 733.
[2] Y.T. Oganessian, F.S. Abdullin, P.D. Bailey, et al., Phys. Rev. Lett. 104 (2010) 142502.
[3] V. Zagrebaev, W. Greiner, Phys. Rev. C 78 (2008) 034610.
[4] G. Adamian, N. Antonenko, A. Diaz-Torres, et al., Nuclear Phys. A 671 (2000) 233.
[5] N. Wang, J. Tian, W. Scheid, Phys. Rev. C 84 (2011) 061601.
[6] V.V. Sargsyan, G.G. Adamian, N.V. Antonenko, et al., Phys. Rev. C 84 (2011) 064614.
[7] W.D. Myers, W.J. Świaątecki, Phys. Rev. C 62 (2000) 044610.
[8] M. Dasgupta, D. Hinde, N. Rowley, et al., Annu. Rev. Nucl. Part. S 48 (1998) 401.
[9] T. Ichikawa, Phys. Rev. C 92 (2015) 064604.
[10] P.W. Wen, C.J. Lin, R.G. Nazmitdinov, et al., Phys. Rev. C 103 (2021) 054601.
[11] G. Gamow, Z. Phys. 51 (1928) 204.
[12] C.Y. Wong, Phys. Rev. Lett. 31 (1973) 766.
[13] V. Yu Denisov, I. Yu Sedykh, Eur. Phys. J. A 55 (2019) 153.
[14] P. Stelson, Phys. Lett. B 205 (1988) 190.
[15] P.H. Stelson, H.J. Kim, M. Beckerman, et al., Phys. Rev. C 41 (1990) 1584.
[16] K. Siwek-Wilczyńska, J. Wilczyński, Phys. Rev. C 69 (2004) 024611.
[17] C.L. Jiang, K.E. Rehm, B.B. Back, et al., Eur. Phys. J. A 54 (2018) 218.
[18] P.W. Wen, C.J. Lin, H.M. Jia, et al., Phys. Rev. C 105 (2022) 034606.
[19] M. Liu, N. Wang, Z. Li, et al., Nuclear Phys. A 768 (2006) 80.
[20] N. Wang, M. Liu, Y. Yang, Sci. China Ser. G-Phys. Mech. Astron. 52 (2009) 1554.
[21] V.I. Zagrebaev, Y. Aritomo, M.G. Itkis, et al., Phys. Rev. C 65 (2001) 014607.
[22] B. Wang, K. Wen, W.-J. Zhao, et al., At. Data Nucl. Data Tables 114 (2017) 281.
[23] N. Wang, Z. Li, W. Scheid, J. Phys. G: Nucl. Part. Phys. 34 (2007) 1935.
[24] C.L. Jiang, B.P. Kay, Phys. Rev. C 105 (2022) 064601.
[25] N. Rowley, G. Satchler, P. Stelson, Phys. Lett. B 254 (1991) 25.
[26] H. Timmers, D. Ackermann, S. Beghini, et al., Nuclear Phys. A 633 (1998) 421.
[27] J.R. Birkelund, J.R. Huizenga, Phys. Rev. C 17 (1978) 126.
[28] K. Washiyama, D. Lacroix, Phys. Rev. C 78 (2008) 024610.
[29] H.B. Zhou, Z.Y. Li, Z.G. Gan, et al., Phys. Rev. C 105 (2022) 024328.
[30] Y. Jiang, N. Wang, Z. Li, et al., Phys. Rev. C 81 (2010) 044602.
[31] N. Wang, L. Ou, Y. Zhang, et al., Phys. Rev. C 89 (2014) 064601.
[32] A.S. Umar, V.E. Oberacker, Phys. Rev. C 74 (2006) 021601.
[33] C.R. Morton, A.C. Berriman, M. Dasgupta, et al., Phys. Rev. C 60 (1999) 044608.
[34] C.R. Morton, A.C. Berriman, R.D. Butt, et al., Phys. Rev. C 62 (2000) 024607.
[35] A.S. Umar, V.E. Oberacker, J.A. Maruhn, et al., Phys. Rev. C 80 (2009) 041601.
[36] N. Rowley, K. Hagino, Phys. Rev. C 91 (2015) 044617.
[37] H.Q. Zhang, C.J. Lin, F. Yang, et al., Phys. Rev. C 82 (2010) 054609.
[38] A.M. Stefanini, D. Ackermann, L. Corradi, et al., Phys. Rev. C 52 (1995) R1727.
[39] F. James, M. Roos, Comput. Phys. Comm. 10 (1975) 343.
[40] A.M. Stefanini, G. Montagnoli, L. Corradi, et al., Phys. Rev. C 82 (2010) 014614.
[41] A.M. Stefanini, D. Ackermann, L. Corradi, et al., Phys. Rev. Lett. 74 (1995) 864.
[42] http://nrv.jinr.ru/nrv/.
[43] W. Swiatecki, Nuclear Phys. A 376 (1982) 275.
[44] N. Wang, T. Li, Phys. Rev. C 88 (2013) 011301.
[45] I. Angeli, K.P. Marinova, At. Data Nucl. Data Tables 99 (2013) 69.
[46] T. Li, Y. Luo, N. Wang, At. Data Nucl. Data Tables 140 (2021) 101440.
[47] W.J. Świątecki, K. Siwek-Wilczyńska, J. Wilczyński, Phys. Rev. C 71 (2005) 014602.
[48] R. Bock, Y. Chu, M. Dakowski, et al., Nuclear Phys. A 388 (1982) 334.
[49] C.S. Palshetkar, S. Santra, A. Chatterjee, et al., Phys. Rev. C 82 (2010) 044608.
[50] S. Gil, R. Vandenbosch, A.J. Lazzarini, et al., Phys. Rev. C 31 (1985) 1752.
[51] H. Freiesleben, J. Huizenga, Nuclear Phys. A 224 (1974) 503.
[52] R. Gunnink, J.W. Cobble, Phys. Rev. 115 (1959) 1247.
[53] P. Limkilde, G. Sletten, Nuclear Phys. A 199 (1973) 504.
[54] L.J. Colby, M.L. Shoaf, J.W. Cobble, Phys. Rev. 121 (1961) 1415.
[55] A. Fleury, F.H. Ruddy, M.N. Namboodiri, et al., Phys. Rev. C 7 (1973) 1231.
[56] M. Fisichella, V. Scuderi, A. Di Pietro, et al., J. Phys. Conf. Ser. 282 (2011) 012014.
[57] J.J. Kolata, V. Guimarães, D. Peterson, et al., Phys. Rev. Lett. 81 (1998) 4580.
[58] A. Lemasson, A. Shrivastava, A. Navin, et al., Phys. Rev. Lett. 103 (2009) 232701.
[59] M.M. Shaikh, S. Roy, S. Rajbanshi, et al., Phys. Rev. C 91 (2015) 034615.
[60] A. Di Pietro, P. Figuera, E. Strano, et al., Phys. Rev. C 87 (2013) 064614.
[61] H. Kumawat, V. Jha, V.V. Parkar, et al., Phys. Rev. C 86 (2012) 024607.
[62] P.K. Rath, S. Santra, N.L. Singh, et al., Phys. Rev. C 79 (2009) 051601.
[63] P. Rath, S. Santra, N. Singh, et al., Nuclear Phys. A 874 (2012) 14.
[64] M.K. Pradhan, A. Mukherjee, P. Basu, et al., Phys. Rev. C 83 (2011) 064606.
[65] A. Shrivastava, A. Navin, A. Lemasson, et al., Phys. Rev. Lett. 103 (2009) 232702.
[66] C.S. Palshetkar, S. Thakur, V. Nanal, et al., Phys. Rev. C 89 (2014) 024607.
[67] M. Dasgupta, D.J. Hinde, K. Hagino, et al., Phys. Rev. C 66 (2002) 041602.
[68] H. Freiesleben, G.T. Rizzo, J.R. Huizenga, Phys. Rev. C 12 (1975) 42.
[69] C. Scholz, L. Ricken, E. Kuhlmann, Z. Phys. A 325 (1986) 203.
[70] A. Pakou, K. Rusek, N. Alamanos, et al., Eur. Phys. J. A 39 (2009) 187.
[71] C. Beck, F.A. Souza, N. Rowley, et al., Phys. Rev. C 67 (2003) 054602.
[72] P.K. Rath, S. Santra, N.L. Singh, et al., Phys. Rev. C 88 (2013) 044617.
[73] R. Broda, M. Ishihara, B. Herskind, et al., Nuclear Phys. A 248 (1975) 356.
[74] A. Shrivastava, A. Navin, A. Diaz-Torres, et al., Phys. Lett. B 718 (2013) 931.
[75] H. Freiesleben, H.C. Britt, J. Birkelund, et al., Phys. Rev. C 10 (1974) 245.
[76] A. Parihari, S. Santra, A. Pal, et al., Phys. Rev. C 90 (2014) 014603.
[77] E. Martinez-Quiroz, E.F. Aguilera, D. Lizcano, et al., Phys. Rev. C 90 (2014) 014616.
[78] R. Raabe, C. Angulo, J.L. Charvet, et al., Phys. Rev. C 74 (2006) 044606.
[79] V.V. Parkar, R. Palit, S.K. Sharma, et al., Phys. Rev. C 82 (2010) 054601.
[80] P.R.S. Gomes, I. Padron, E. Crema, et al., Phys. Rev. C 73 (2006) 064606.
[81] Y.D. Fang, P.R.S. Gomes, J. Lubian, et al., Phys. Rev. C 91 (2015) 014608.
[82] N.T. Zhang, Y.D. Fang, P.R.S. Gomes, et al., Phys. Rev. C 90 (2014) 024621.
[83] M. Dasgupta, P.R.S. Gomes, D.J. Hinde, et al., Phys. Rev. C 70 (2004) 024606.
[84] Z. Liu, C. Signorini, M. Mazzocco, et al., Eur. Phys. J. A 26 (2005) 73.
[85] C. Signorini, Z. Liu, Z. Li, et al., Eur. Phys. J. A 5 (1999) 7.
[86] C. Signorini, Z. Liu, A. Yoshida, et al., Eur. Phys. J. A 2 (1998) 227.
[87] A. Mukherjee, Subinit Roy, M. Pradhan, et al., Phys. Lett. B 636 (2006) 91.
[88] B. Dasmahapatra, B. Čujec, F. Lahlou, Nuclear Phys. A 408 (1983) 192.
[89] Z. Liu, H. Zhang, J. Xu, et al., Phys. Rev. C 54 (1996) 761.
[90] H. Cheung, M. High, B. Čujec, Nuclear Phys. A 296 (1978) 333.
[91] M. High, B. Čujec, Nuclear Phys. A 278 (1977) 149.
[92] R.G. Stokstad, Z.E. Switkowski, R.A. Dayras, et al., Phys. Rev. Lett. 37 (1976) 888.
[93] B. Dasmahapatra, B. Čujec, Nuclear Phys. A 565 (1993) 657.
[94] G. Hulke, C. Rolfs, H. Trautvetter, Z. Phys. A 297 (1980) 161.
[95] E. Bozek, D. De Castro-Rizzo, S. Cavallaro, et al., Nuclear Phys. A 451 (1986) 171.
[96] J.O. Newton, C.R. Morton, M. Dasgupta, et al., Phys. Rev. C 64 (2001) 064608.

[97] D. Abriola, A.A. Sonzogni, M. di Tada, et al., Phys. Rev. C 46 (1992) 244.
[98] M. Crippa, E. Gadioli, P. Vergani, et al., Z. Phys. A 350 (1994) 121.
[99] A. Shrivastava, S. Kailas, A. Chatterjee, et al., Phys. Rev. C 63 (2001) 054602.
[100] R.N. Sagaidak, G.N. Kniajeva, I.M. Itkis, et al., Phys. Rev. C 68 (2003) 014603.
[101] A. Mukherjee, D.J. Hinde, M. Dasgupta, et al., Phys. Rev. C 75 (2007) 044608.
[102] M.L. Chatterjee, L. Potvin, B. Čujec, Nuclear Phys. A 333 (1980) 273.
[103] H. Dumont, B. Delaunay, J. Delaunay, et al., Nuclear Phys. A 435 (1985) 301.
[104] B.P. Ajith Kumar, K.M. Varier, R.G. Thomas, et al., Phys. Rev. C 72 (2005) 067601.
[105] Shiu-Chin Wu, J. Overley, C. Barnes, et al., Nuclear Phys. A 312 (1978) 177.
[106] Z. Switkowski, R. Stokstad, R. Wieland, Nuclear Phys. A 279 (1977) 502.
[107] P.A. DeYoung, J.J. Kolata, L.J. Satkowiak, et al., Phys. Rev. C 26 (1982) 1482.
[108] Z. Switkowski, R. Stokstad, R. Wieland, Nuclear Phys. A 274 (1976) 202.
[109] P. Gomes, T. Penna, R. Liguori Neto, et al., Nucl. Instrum. Methods A 280 (1989) 395.
[110] B.R. Behera, M. Satpathy, S. Jena, et al., Phys. Rev. C 69 (2004) 064603.
[111] H. Funaki, E. Arai, Nuclear Phys. A 556 (1993) 307.
[112] E. Vulgaris, L. Grodzins, S.G. Steadman, et al., Phys. Rev. C 33 (1986) 2017.
[113] P. Christensen, Z. Switkowskiw, R. Dayras, Nuclear Phys. A 280 (1977) 189.
[114] B. Dasmahapatra, B. Čujec, I. Szöghy, et al., Nuclear Phys. A 526 (1991) 395.
[115] A. Kuronen, J. Keinonen, P. Tikkanen, Phys. Rev. C 35 (1987) 591.
[116] J. Thomas, Y.T. Chen, S. Hinds, et al., Phys. Rev. C 33 (1986) 1679.
[117] J. Dauk, K. Lieb, A. Kleinfeld, Nuclear Phys. A 241 (1975) 170.
[118] R.L. Neto, J. Acquadro, P. Gomes, et al., Nuclear Phys. A 512 (1990) 333.
[119] N. Keeley, J. Lilley, J. Wei, et al., Nuclear Phys. A 628 (1998) 1.
[120] L. Chamon, D. Pereira, E. Rossi, et al., Phys. Lett. B 275 (1992) 29.
[121] D. Pereira, G. Ramirez, O. Sala, et al., Phys. Lett. B 220 (1989) 347.
[122] M. Langevin, J. Barreto, C. Détraz, Phys. Rev. C 14 (1976) 152.
[123] P.R.S. Gomes, M.D. Rodríguez, G.V. Martí, et al., Phys. Rev. C 71 (2005) 034608.
[124] E.F. Aguilera, J.J. Kolata, R.J. Tighe, Phys. Rev. C 52 (1995) 3103.
[125] H.M. Jia, C.J. Lin, F. Yang, et al., Phys. Rev. C 86 (2012) 044621.
[126] D. Ackermann, L. Corradi, D. Napoli, et al., Nuclear Phys. A 575 (1994) 374.
[127] V. Tripathi, L.T. Baby, J.J. Das, et al., Phys. Rev. C 65 (2001) 014614.
[128] M. di Tada, D.E. DiGregorio, D. Abriola, et al., Phys. Rev. C 47 (1993) 2970.
[129] J.R. Leigh, M. Dasgupta, D.J. Hinde, et al., Phys. Rev. C 52 (1995) 3151.
[130] D.E. DiGregorio, M. diTada, D. Abriola, et al., Phys. Rev. C 39 (1989) 516.
[131] R.G. Stokstad, Y. Eisen, S. Kaplanis, et al., Phys. Rev. C 21 (1980) 2427.
[132] U. Jahnke, H. Rossner, D. Hilscher, et al., Phys. Rev. Lett. 48 (1982) 17.
[133] J.X. Wei, J.R. Leigh, D.J. Hinde, et al., Phys. Rev. Lett. 67 (1991) 3368.
[134] J.O. Fernández Niello, M. di Tada, A.O. Macchiavelli, et al., Phys. Rev. C 43 (1991) 2303.
[135] T. Rajbongshi, K. Kalita, S. Nath, et al., Phys. Rev. C 93 (2016) 054622.
[136] R. Lemmon, J. Leigh, J. Wei, et al., Phys. Lett. B 316 (1993) 32.
[137] M. Trotta, A. Stefanini, S. Beghini, et al., Eur. Phys. J. A 25 (2005) 615.
[138] E. Prasad, K. Varier, R. Thomas, et al., Nuclear Phys. A 882 (2012) 62.
[139] E. Prasad, K.M. Varier, N. Madhavan, et al., Phys. Rev. C 84 (2011) 064606.
[140] T. Sikkeland, Phys. Rev. 135 (1964) B669.
[141] Y. Eyal, M. Beckerman, R. Chechik, et al., Phys. Rev. C 13 (1976) 1527.
[142] R.J. Tighe, J.J. Kolata, M. Belbot, et al., Phys. Rev. C 47 (1993) 2699.
[143] H. Roth, J. Christiansson, J. Dubois, Nuclear Phys. A 343 (1980) 148.
[144] T.K. Steinbach, J. Vadas, J. Schmidt, et al., Phys. Rev. C 90 (2014) 041603.
[145] A.M. Borges, C.P. da Silva, D. Pereira, et al., Phys. Rev. C 46 (1992) 2360.
[146] C.P. Silva, D. Pereira, L.C. Chamon, et al., Phys. Rev. C 55 (1997) 3155.
[147] N.V. Prasad, A. Vinodkumar, A. Sinha, et al., Nuclear Phys. A 603 (1996).
[148] D. Hinde, J. Leigh, J. Newton, et al., Nuclear Phys. A 385 (1982) 109.
[149] K. Mahata, S. Kailas, A. Shrivastava, et al., Nuclear Phys. A 720 (2003) 209.
[150] D.J. Hinde, A.C. Berriman, M. Dasgupta, et al., Phys. Rev. C 60 (1999) 054602.
[151] Z. Huanqiao, L. Zuhua, X. Jincheng, et al., Nuclear Phys. A 512 (1990) 531.
[152] K.E. Rehm, H. Esbensen, C.L. Jiang, et al., Phys. Rev. Lett. 81 (1998) 3341.
[153] A. Samant, S. Kailas, A. Chatterjee, et al., Eur. Phys. J. A 7 (2000) 59.
[154] N. Majumdar, P. Bhattacharya, D.C. Biswas, et al., Phys. Rev. C 51 (1995) 3109.
[155] S. Kailas, A. Navin, A. Chatterjee, et al., Phys. Rev. C 43 (1991) 1466.
[156] H. Zhang, J. Xu, Z. Liu, et al., Phys. Lett. B 218 (1989) 133.
[157] E. Piasecki, L. Świderski, N. Keeley, et al., Phys. Rev. C 85 (2012) 054608.
[158] V.E. Viola, T. Sikkeland, Phys. Rev. 128 (1962) 767.
[159] R. Butsch, H. Jänsch, D. Krämer, et al., Phys. Rev. Lett. 57 (1986) 2002.
[160] S. Gary, C. Volant, Phys. Rev. C 25 (1982) 1877.
[161] C.L. Jiang, A.M. Stefanini, H. Esbensen, et al., Phys. Rev. Lett. 113 (2014) 022701.
[162] M. Itkis, I. Itkis, G. Knyazheva, et al., Nuclear Phys. A 834 (2010) 374c.
[163] C.L. Jiang, K.E. Rehm, H. Esbensen, et al., Phys. Rev. C 81 (2010) 024611.
[164] E.F. Aguilera, J.J. Vega, J.J. Kolata, et al., Phys. Rev. C 41 (1990) 910.
[165] Y. Watanabe, A. Yoshida, T. Fukuda, et al., Eur. Phys. J. A 10 (2001) 373.
[166] A. Morsad, J.J. Kolata, R.J. Tighe, et al., Phys. Rev. C 41 (1990) 988.
[167] G. Montagnoli, A.M. Stefanini, H. Esbensen, et al., Phys. Rev. C 90 (2014) 044608.
[168] C.L. Jiang, B.B. Back, H. Esbensen, et al., Phys. Rev. C 78 (2008) 017601.
[169] A.M. Stefanini, G. Fortuna, A. Tivelli, et al., Phys. Rev. C 30 (1984) 2088.
[170] A. Stefanini, G. Fortuna, R. Pengo, et al., Nuclear Phys. A 456 (1986) 509.
[171] C. Jiang, B. Back, H. Esbensen, et al., Phys. Lett. B 640 (2006) 18.
[172] A.K. Sinha, L.T. Baby, N. Badiger, et al., J. Phys. G: Nucl. Part. Phys. 23 (1997) 1331.
[173] M. Dasgupta, A. Navin, Y.K. Agarwal, et al., Nuclear Phys. A 539 (1992) 351.
[174] M. Dasgupta, A. Navin, Y.K. Agarwal, et al., Phys. Rev. Lett. 66 (1991) 1414.
[175] S. Kalkal, S. Mandal, N. Madhavan, et al., Phys. Rev. C 81 (2010) 044610.
[176] Khushboo S. Mandal, S. Nath, et al., Phys. Rev. C 96 (2017) 014614.
[177] L.T. Baby, V. Tripathi, D.O. Kataria, et al., Phys. Rev. C 56 (1997) 1936.
[178] D. Ackermann, P. Bednarczyk, L. Corradi, et al., Nuclear Phys. A 609 (1996) 91.
[179] D. Ackermann, F. Scarlassara, P. Bednarczyk, et al., Nuclear Phys. A 583 (1995) 129.
[180] S. Gil, D. Abriola, D.E. DiGregorio, et al., Phys. Rev. Lett. 65 (1990) 3100.
[181] D. Hinde, R. Charity, G. Foote, et al., Nuclear Phys. A 452 (1986) 550.
[182] R.D. Butt, D.J. Hinde, M. Dasgupta, et al., Phys. Rev. C 66 (2002) 044601.
[183] K. Nishio, H. Ikezoe, S. Mitsuoka, et al., Phys. Rev. C 62 (2000) 014602.
[184] D. Hinde, C. Morton, M. Dasgupta, et al., Nuclear Phys. A 592 (1995) 271.
[185] K. Nishio, S. Hofmann, F. Heßberger, et al., Eur. Phys. J. A 29 (2006) 281.
[186] K. Nishio, H. Ikezoe, I. Nishinaka, et al., Phys. Rev. C 82 (2010) 044604.
[187] A. Menchaca-Rocha, E. Belmont-Moreno, M.E. Brandan, et al., Phys. Rev. C 41 (1990) 2654.
[188] G.M. Berkowitz, P. Braun-Munzinger, J.S. Karp, et al., Phys. Rev. C 28 (1983) 667.
[189] G. Montagnoli, A.M. Stefanini, H. Esbensen, et al., Phys. Rev. C 87 (2013) 014611.
[190] R.J. Tighe, J.J. Vega, E. Aguilera, et al., Phys. Rev. C 42 (1990) 1530.
[191] A. Stefanini, G. Fortuna, R. Pengo, et al., Phys. Lett. B 162 (1985) 66.
[192] A. Mukherjee, M. Dasgupta, D.J. Hinde, et al., Phys. Rev. C 66 (2002) 034607.
[193] H.M. Jia, C.J. Lin, F. Yang, et al., Phys. Rev. C 89 (2014) 064605.
[194] R. Pengo, D. Evers, K. Löbner, et al., Nuclear Phys. A 411 (1983) 255.
[195] S. Gil, F. Hasenbalg, J.E. Testoni, et al., Phys. Rev. C 51 (1995) 1336.
[196] P.R.S. Gomes, I.C. Charret, R. Wanis, et al., Phys. Rev. C 49 (1994) 245.
[197] S. Mitsuoka, H. Ikezoe, K. Nishio, et al., Phys. Rev. C 62 (2000) 054603.
[198] H. Zhang, C. Zhang, C. Lin, et al., J. Phys. Conf. Ser. 282 (2011) 012013.
[199] B.B. Back, D.J. Blumenthal, C.N. Davids, et al., Phys. Rev. C 60 (1999) 044602.
[200] L. Corradi, S. Skorka, U. Lenz, et al., Z. Phys. A 335 (1990) 55.
[201] C. Morton, D. Hinde, A. Berriman, et al., Phys. Lett. B 481 (2000) 160.
[202] J. Khuyagbaatar, K. Nishio, S. Hofmann, et al., Phys. Rev. C 86 (2012) 064602.
[203] K. Nishio, S. Hofmann, F.P. Heßberger, et al., Phys. Rev. C 82 (2010) 024611.
[204] A.M. Stefanini, G. Montagnoli, R. Silvestri, et al., Phys. Rev. C 78 (2008) 044607.
[205] G. Montagnoli, S. Beghini, B. Guiot, et al., AIP Conf. Proc. 1098 (2009) 38.
[206] G. Montagnoli, A.M. Stefanini, L. Corradi, et al., Phys. Rev. C 82 (2010) 064609.
[207] A.M. Stefanini, L. Corradi, A.M. Vinodkumar, et al., Phys. Rev. C 62 (2000) 014601.
[208] S. Cavallaro, M. Sperduto, B. Delaunay, et al., Nuclear Phys. A 513 (1990) 174.
[209] W. Scobel, H.H. Gutbrod, M. Blann, et al., Phys. Rev. C 14 (1976) 1808.
[210] E.M. Szanto, R.L. Neto, M.C.S. Figueira, et al., Phys. Rev. C 41 (1990) 2164.
[211] W. Scobel, A. Mignerey, M. Blann, et al., Phys. Rev. C 11 (1975) 1701.
[212] R.N. Sahoo, M. Kaushik, A. Sood, et al., Phys. Rev. C 102 (2020) 024615.
[213] E. Martínez-Quiroz, E.F. Aguilera, J.J. Kolata, et al., Phys. Rev. C 63 (2001) 054611.
[214] J. Mahon, L. Lee Jr., J. Liang, et al., J. Phys. G: Nucl. Part. Phys. 23 (1997) 1215.
[215] W. Reisdorf, F. Hessberger, K. Hildenbrand, et al., Nuclear Phys. A 438 (1985) 212.
[216] R. Stokstad, W. Reisdorf, K. Hildenbrand, et al., Z. Phys. A 295 (1980) 269.
[217] H.-G. Clerc, J. Keller, C.-C. Sahm, et al., Nuclear Phys. A 419 (1984) 571.
[218] H.A. Aljuwair, R.J. Ledoux, M. Beckerman, et al., Phys. Rev. C 30 (1984) 1223.

[219] G. Montagnoli, A.M. Stefanini, C.L. Jiang, et al., Phys. Rev. C 85 (2012) 024607.
[220] C.L. Jiang, A.M. Stefanini, H. Esbensen, et al., Phys. Rev. C 82 (2010) 041601.
[221] M. Trotta, A.M. Stefanini, L. Corradi, et al., Phys. Rev. C 65 (2001) 011601.
[222] R. Vandenbosch, A.A. Sonzogni, J.D. Bierman, J. Phys. G: Nucl. Part. Phys. 23 (1997) 1303.
[223] B. Sikora, J. Bisplinghoff, W. Scobel, et al., Phys. Rev. C 20 (1979) 2219.
[224] D. Bourgin, S. Courtin, F. Haas, et al., Phys. Rev. C 90 (2014) 044610.
[225] H. Timmers, L. Corradi, A. Stefanini, et al., Phys. Lett. B 399 (1997) 35.
[226] A.M. Stefanini, B.R. Behera, S. Beghini, et al., Phys. Rev. C 76 (2007) 014610.
[227] A. Stefanini, G. Montagnoli, H. Esbensen, et al., Phys. Lett. B 728 (2014) 639.
[228] A.M. Stefanini, J. Phys. G: Nucl. Part. Phys. 23 (1997) 1401.
[229] F. Scarlassara, S. Beghini, G. Montagnoli, et al., Nuclear Phys. A 672 (2000) 99.
[230] J.D. Bierman, P. Chan, J.F. Liang, et al., Phys. Rev. C 54 (1996) 3068.
[231] A.J. Pacheco, J.O. Fernández Niello, D.E. DiGregorio, et al., Phys. Rev. C 45 (1992) 2861.
[232] K. Nishio, S. Mitsuoka, I. Nishinaka, et al., Phys. Rev. C 86 (2012) 034608.
[233] A. Stefanini, G. Montagnoli, R. Silvestri, et al., Phys. Lett. B 679 (2009) 95.
[234] A.M. Stefanini, F. Scarlassara, S. Beghini, et al., Phys. Rev. C 73 (2006) 034606.
[235] M. Trotta, A. Stefanini, L. Corradi, et al., Nuclear Phys. A 734 (2004) 245.
[236] A. Stefanini, M. Trotta, B. Behera, et al., Eur. Phys. J. A 23 (2005) 473.
[237] E. Prokhorova, A. Bogachev, M. Itkis, et al., Nuclear Phys. A 802 (2008) 45.
[238] A.M. Stefanini, M. Trotta, L. Corradi, et al., Phys. Rev. C 65 (2002) 034609.
[239] A.M. Stefanini, G. Montagnoli, L. Corradi, et al., Phys. Rev. C 92 (2015) 064607.
[240] A.M. Vinodkumar, K.M. Varier, N.V.S.V. Prasad, et al., Phys. Rev. C 53 (1996) 803.
[241] A.M. Stefanini, G. Montagnoli, L. Corradi, et al., Phys. Rev. C 81 (2010) 037601.
[242] M. Beckerman, J. Ball, H. Enge, et al., Phys. Rev. C 23 (1981) 1581.
[243] M. Beckerman, M. Salomaa, A. Sperduto, et al., Phys. Rev. Lett. 45 (1980) 1472.
[244] M. Beckerman, M. Salomaa, A. Sperduto, et al., Phys. Rev. C 25 (1982) 837.
[245] F. Scarlassara, S. Beghini, F. Soramel, et al., Z. Phys. A 338 (1991) 171.
[246] K. Rehm, H. Esbensen, J. Gehring, et al., Phys. Lett. B 317 (1993) 31.
[247] F.L.H. Wolfs, Phys. Rev. C 36 (1987) 1379.
[248] K.T. Lesko, W. Henning, K.E. Rehm, et al., Phys. Rev. C 34 (1986) 2155.
[249] C.L. Jiang, A.M. Stefanini, H. Esbensen, et al., Phys. Rev. C 91 (2015) 044602.
[250] C.L. Jiang, H. Esbensen, K.E. Rehm, et al., Phys. Rev. Lett. 89 (2002) 052701.
[251] A. Stefanini, G. Montagnoli, F. Scarlassara, et al., Eur. Phys. J. A 49 (2013) 1.
[252] C.L. Jiang, K.E. Rehm, R.V.F. Janssens, et al., Phys. Rev. Lett. 93 (2004) 012701.
[253] A. Stefanini, L. Corradi, D. Ackermann, et al., Nuclear Phys. A 548 (1992) 453.
[254] W.S. Freeman, H. Ernst, D.F. Geesaman, et al., Phys. Rev. Lett. 50 (1983) 1563.
[255] K.T. Lesko, W. Henning, K.E. Rehm, et al., Phys. Rev. Lett. 55 (1985) 803.
[256] M. Beckerman, M.K. Salomaa, J. Wiggins, et al., Phys. Rev. C 28 (1983) 1963.
[257] M. Beckerman, J. Wiggins, H. Aljuwair, et al., Phys. Rev. C 29 (1984) 1938.
[258] W. Reisdorf, F. Hessberger, K. Hildenbrand, et al., Nuclear Phys. A 444 (1985) 154.
[259] J.J. Kolata, A. Roberts, A.M. Howard, et al., Phys. Rev. C 85 (2012) 054603.
[260] Z. Kohley, J.F. Liang, D. Shapira, et al., Phys. Rev. Lett. 107 (2011) 202701.
[261] J. Liang, D. Shapira, C. Gross, et al., Nuclear Phys. A (2004) 103.
[262] J.F. Liang, D. Shapira, J.R. Beene, et al., Phys. Rev. C 75 (2007) 054607.
[263] Z. Kohley, J.F. Liang, D. Shapira, et al., Phys. Rev. C 87 (2013) 064612.
[264] D. Shapira, J. Liang, C. Gross, et al., Eur. Phys. J. A 25 (2005) 241.